ABSTRACT

Alfred Oliver Inman III. AN ULTRASTRUCTURAL STUDY OF
CULICINOMYCES CLAVOSPORUS, A PARASITE OF MOSQUITOS AND
RELATED DIPTERA. (Under the direction of Dr. Charles
Bland), Department of Biology, East Carolina University.
December, 1981.

Studies were conducted via light and electron microscopy
to determine, relative to the biology of Culicinomyces
clavosporus, the following: (1) ultrastructure of the
conidium; (2) infection of mosquito larvae (Aedes aegypti
and A. taeniorhynchus); (3) host/parasite interactions at
the cellular level; and (4) fungal conidiogenesis.

Larvae become infected by submerged conidia through the
cuticle of the foregut and hindgut and, when exposed to high
concentrations of conidia (10^4-10^6 conidia/ml), through the
epicuticle of the anal gills as well. As the fungus grows
throughout the hemocoel, larval movements become increasingly
sluggish. Hyphae grow to completely pack the anal gills about
the time of larval death and subsequently rupture the thin
epicuticle. Following this, the abdomen, thorax, and head
become packed with hyphae. Hyphae then rupture the epicuticle
in all regions but the head and siphon. Within 24 hours,
conidia are formed on the emergent vegetative hyphae.

AN ULTRASTRUCTURAL STUDY OF <u>CULICINOMYCES CLAVOSPORUS</u>,

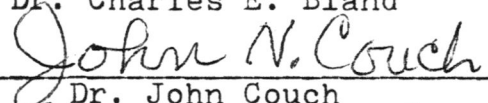A PARASITE OF MOSQUITOS AND RELATED DIPTERA

by

Alfred O. Inman III

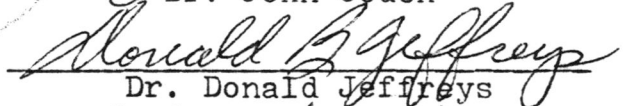APPROVED BY:

    SUPERVISOR OF THESIS   *Charles E. Bland*
                                      Dr. Charles E. Bland

    THESIS COMMITTEE   *John N. Couch*
                                        Dr. John Couch

                                   Donald B. Jeffreys
                                    Dr. Donald Jeffreys

                                   Clifford Knight
                                    Dr. Clifford Knight
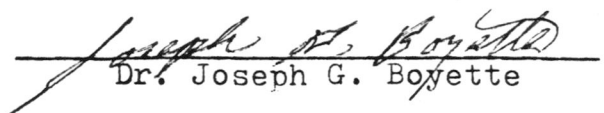
    CHAIRMAN OF THE DEPARTMENT OF BIOLOGY
                                  Charles E. Bland
                                    Dr. Charles E. Bland

    DEAN OF THE GRADUATE SCHOOL

                               Joseph G. Boyette
                                Dr. Joseph G. Boyette

AN ULTRASTRUCTURAL STUDY OF <u>CULICINOMYCES</u> <u>CLAVOSPORUS</u>,

A PARASITE OF MOSQUITOS AND RELATED DIPTERA

A Thesis

Presented to

the Faculty of the Department of Biology

East Carolina University

In Partial Fulfillment

of the Requirements for the Degree

Master of Science in Biology

by

Alfred O. Inman III

December, 1981

ACKNOWLEDGMENTS

TABLE OF CONTENTS

ABBREVIATIONS

A - autophagosome

Ab - abdomen

Ag - anal gills

Am - amorphous material

Ap - anal pore

b - bacterium

C - collar

Ca - cavity

Cc - conidiogenous cell

Ci - conidial initial

Cl - conidiogenous locus

Cm - conidium

Co - collarette

Cw - conidial wall

dbv - dense body vacuole

dcv - dense core vesicle

dl - dense wall layer

Ep - epicuticle

ER - endoplasmic reticulum

f - wall fracture

fs - fibrous sphere

gb - granular body

GC - gut cuticle

gr - granular region

GT - germ tube

GTi - germ tube initial

H - hypha

HC - hyphal cell

He - head

Is - intersegmental region

L - lipid body

Lu - lumen of gut

M - mitochondrion

mc - mucilaginous coat

Me - melanization

mf - microfilament

mvc - multivesicular complex

N - nucleus

No - nucleolus

ov - opaque vesicle

Ph - penetrant hypha

Pl - phospholipid body

pls - irregular plasmalemmasome

pm - plasma membrane

pwl - primary wall layer

R - ribosomes

RB - residual body

RER - rough endoplasmic reticulum

rep - ruptured epicuticle

rp - ribosome packet

sbp - subbasal peg

se - septum

SER - smooth endoplasmic reticulum

Si - siphon

sp - septal pore

spl - septal plug

st - sterigma

swl - secondary wall layer

Th - thorax

tl - translucent wall layer

twl - tertiary wall layer

V - vacuole

vh - vegetative hypha

W - Woronin body

wps - whorled plasmalemmasome

wr - wall remnants

INTRODUCTION

Culicinomyces clavosporus Couch (1974), a member of the
class Deuteromycetes, was described originally as a parasite
of larvae of the mosquito Anopheles quadrimaculatus Say
collected from University Lake, Chapel Hill, North Carolina.
Sweeney et. al. (1973), working in Australia, discovered and
subsequently described an apparently con-specific fungus
parasitizing larvae in a laboratory colony of Anopheles
amictus hilli Woodhill and Lee. In this situation, it was
felt that the fungus was introduced in water from McCarr's
Creek, French Forest Sidney, which was used in the laboratory
culture of mosquito larvae. Both the American and Australian
strains of C. clavosporus are similar morphologically in being
characterized by hyaline, branched hyphae with flask-shaped,
one to several times septate primary conidiogenous cells
from which arise hyaline, club-shaped or obclavate, nonseptate
conidia. Primary conidia are generally larger than later
ones.

Sweeney (1975a) reported that during infection conidia
ingested by larvae of Culex fatigans adhere longitudinally
to the gut cuticle in the foregut and hindgut regions.
Germination is at the narrow, anteriorly directed apex of
attached conidia and occurs via a slender germ tube which
pierces the integument. Following penetration, the germ
tube (penetrant hypha) swells into an oval to spherical cell
upon reaching the hemocoel. Proliferation of hyphae and

hyphal bodies from the cell results in fungal invasion of the entire hemocoel of the host. Continued growth of the fungus results in depletion of host body tissue and ultimately in death. Following death, the hemocoel becomes packed with hyphae that subsequently ruptures the cuticle of the abdomen and thorax. Sporulation (conidial formation) occurs 1-2 days following death (Sweeney, 1975a). In addition to infection through the gut, later studies (Sweeney, 1979b) have shown that when larvae are subjected to high concentrations of conidia (10^4-10^6 conidia/ml), infection may also occur through the anal gills. Under conditions involving multiple infection sites, 100% mortality of the larvae in a given population would occur.

In limited studies involving $\underline{C}$. $\underline{clavosporus}$, Sweeney (1978a,b) showed that host infection varied with both temperature and salinity of the water at larval breeding sites. In this regard, infection has been noted at temperatures ranging from 15-27.5°C. However, at 30°C the larvae moulted prior to hemocoel invasion and no infection occurred. Although the fungus appears to be nonpathogenic in undiluted sea water, it is fatal to larvae raised in water at half that salinity.

The host range of $\underline{C}$. $\underline{clavosporus}$ is limited to aquatic larvae of certain families of the order Diptera (Sweeney, 1975a, 1979). This order includes midges (Chironomidae), biting midges (Ceratopogonidae), and black flies (Simuliidae),

as well as mosquitos (Culicidae). Preliminary studies on
rats, mice, guinea pigs, sheep, cattle, and ducks indicate
the fungus elicits no allergic response from warm-blooded
animals and is otherwise nontoxic to them (Egerton et. al.,
1978).

The current interest in C. clavosporus is due to its
potential as a biological control agent of mosquitos. In
this regard, the parasite fulfills the following criteria
for a successful biocontrol agent: (1) it rapidly infects
and kills all medically important mosquitos, including the
vector for mammalian malaria (Anopheles); (2) it apparently
elicits no toxic or allergic response to nontarget organisms,
such as warm-blooded animals; (3) it can be cultured
economically on a commercial basis; (4) its conidia do not
lose pathogenicity upon frequent subculturing; and (5) it
is likely to colonize an area once it has been introduced.

As now conceived, biocontrol via C. clavosporus would
augment rather than completely replace chemical insecticides
and natural predators. Initially, the fungus causes little
damage to the environment since it specifically parasitizes
mosquitos. This helps to hold the mosquito population in
check and allows further control by predation. Secondly,
the use of a biological control agent increases the
effectiveness of chemical insecticides and reduces the need
for frequent application. This not only reduces expense but

helps solve the problem of mosquito control in tropical areas where many breeding sources are present.

In using C. clavosporus as a biocontrol agent of mosquitos, two approaches may be taken: short-term control and long-term control. In short-term control, the direct application of heavy concentrations of conidia to an area would provide high larval mortality and would leave few living hosts on which the fungus could propagate. For long-term control, lower concentrations of conidia would be used and would result in moderate mortality rates but continued host availability for propagation of the fungus.

Although several important problems relative to the biology of C. clavosporus have been solved, many others have yet to be seriously addressed, including: (1) Before the fungus can be utilized as a control agent, its worldwide abundance and geographical distribution in the aquatic environment should be determined; (2) Large-scale field trials must be carried out to determine pathogenicity under natural conditions, the long and short term affects on the environment, and fungal persistance with regards to its ability to become established in a given area; (3) Innovative means of conidial application must be devised to insure adequate dosages for larval infection.

In order to establish a foundation for such future work, the research described herein was designed to study the following: (1) the mode of larval infection; (2) the

mechanism by which conidia attach to the gut lining and epicuticle prior to infection; (3) the host/parasite interactions at the cellular level; and (4) the pattern of fungal conidiogenesis.

MATERIALS AND METHODS

Organism Used and In Vitro Culture:

The isolate (American strain)* of <u>Culicinomyces</u> <u>clavosporus</u> Couch used in this study was obtained from the American Type Culture Collection (#38490). Culture was on YPSS agar (yeast extract, 4.0g; phosphate, 1.0g; sulfate, 0.5g; and soluble starch, 15.0g) at $23^{\circ}C$ with propagation of the fungus via hyphal transfer. Both the American strain and an Australian strain (Sweeney, 1973) of <u>C</u>. <u>clavosporus</u> are now maintained in the culture collection of C. E. Bland, Department of Biology, East Carolina University.

In Vivo Culture:

Infection studies were carried out using larvae of <u>Aedes</u> <u>aegypti</u> and <u>Aedes</u> <u>taeniorhynchus</u>. For this, eggs obtained from R. C. Axtell, Department of Entomology, North Carolina State University, were hatched in a fingerbowl containing 200ml of deoxygenated distilled water. Larvae were fed once a day with approximately 0.03g of a 1:1 mixture of Baker's yeast and finely granulated dry dog food.

For infection, viable conidia of <u>C</u>. <u>clavosporus</u> were first collected by washing a 7-14 day old culture with distilled water. The resulting conidial suspension was then diluted to the concentration desired for infection experiments. Larvae (first, second, third, or fourth instar) were then

*Described by Couch (1974)

added to small fingerbowls containing 125 ml of the test suspensions. Larvae exposed to different conidial concentrations were screened by light microscopy at intervals of 24-48 hours to determine the minimal dosage of conidia ensuring high larval mortality and epicuticular infection. By this method larvae were selected at various stages of infection for subsequent study by light and electron microscopy.

Light Microscopy:

To study conidiogenesis, the microchamber technique described by Cole and Kendrick (1968) was modified to ensure optimal growth of the fungus. For this, an agar block cut from a growing colony was placed in the slide chamber between two sterile cover slips, which were in turn cemented to the slide with vaseline. The slide was incubated in a sterile, humid container to help prevent contamination and dessication of the tissue. Under these conditions, hyphae grew in the thin water layer formed on the inside surface of the upper and lower cover slips where conidia formed within 48 hours of inoculation.

Observations of fixed and living material were made with a Zeiss WL microscope equipped with phase-contrast and Nomarski interference contrast optics. All photomicrographs were taken with a Nikon AMF Microflex camera on either Kodak Panatomic X film or Kodak SO 115 Technical Pan film.

Transmission Electron Microscopy:

For studies of larval infection and conidiogenesis via
transmission electron microscopy, specimens were first fixed
at room temperature (23°C) in 3% glutaraldehyde in 0.2 M
cacodylate buffer (pH 7.2) for one hour. To facilitate
penetration of solutions during fixation and further processing,
larvae were cut into three pieces. The tissue was washed in
three 15 minute changes of 0.1 M cacodylate buffer and post-
fixed for one hour in 4% osmic acid buffered in 0.2 M
cacodylate. Specimens were dehydrated for 15 minute intervals
in a graded ethanol series (30%, 50%, 70%, 95%, and 100%),
infiltrated through a transition of propylene oxide and
resin under vacuum (12 psi), and embedded in Araldite 6005
resin. Blocks were cured at 50°C for three days.

Thin sections (600-900Å) were cut on a Reichert OmU2
ultramicrotome with a DuPont diamond knife and collected on
300 mesh copper grids. Sections were stained for five minutes
with saturated uranyl acetate in 50% ethanol and four minutes
in lead citrate (Reynolds, 1963).

The preparations were examined on a Hitachi HS-8
Transmission electron microscope at an accelerating voltage
of 50KV. Micrographs were taken on Kodak Kodalith LR film.

Scanning Electron Microscopy:

Ultrastructural analysis by scanning electron microscopy
was carried out on epicuticular infection, conidiogenesis,
and germination of conidia. To study stages of conidial

germination, conidia washed from 7-14 day old colonies were placed in YPSS broth and agitated on a mechanical shaker (100 rpm) for 2, 11, and 17 hours. Conidia were centrifuged to a pellet, resuspended and rinsed in distilled water, and collected on millipore (0.45 µm) filters. The fixation and dehydration of tissue is the same as described previously. Following dehydration, the tissue was rinsed in amyl acetate (15 min.) and critical point dried in a Technics Critical Point Apparatus using carbon dioxide as the transitional fluid. Specimens were mounted on aluminum stubs with double-stick tape and coated with a gold-palladium alloy in a Technics Hummer V sputter coater.

The preparations were examined with an ISI-40 Scanning electron microscope at accelerating voltages of 10-15 KV. All scanning micrographs were taken on Polaroid Type P/N 55 Land Film.

RESULTS

Laboratory Infection:

Under laboratory conditions, larvae become infected
through the cuticle of the foregut and hindgut and, when
exposed to high concentrations of conidia (10^4- 10^6 conidia/
ml), through the epicuticle of the anal gills as well. As
the fungus grows throughout the hemocoel, larval movements
become increasingly sluggish. About the time of larval
death (approximately 24 hours following conidial adhesion),
hyphae completely fill the anal gills and subsequently rupture
the thin epicuticle. Following this, the abdomen, thorax, and
head become packed with hyphae (approximately 64 hours).
Numerous hyphae then grow through the epicuticle in all regions
but the head and siphon. Within 24 hours of epicuticular
rupture, conidia are formed on the emergent vegetative hyphae.

Structure and Development:

The structure and development of Culicinomyces
clavosporus were studied via light microscopy as well as
transmission and scanning electron microscopy. Results of
these observations will be described in sequence following
the major stages in its life cycle, including: the conidium,
adhesion of conidia to infection sites, germination of conidia,
cuticle penetration, hyphal proliferation and epicuticular
rupture, and conidiogenesis.

The Conidium:

The mature conidium of C. clavosporus is obclavate
(Figures 1, 74, 76, 77, 78, 79, 80, 81, and 82) and measures
1.5-3 x 4-16 µm. It is bound by a bilaminate cell wall
comprised of a 0.1 µm thick electron-translucent, granular,
inner (secondary) layer and a 0.03 µm electron-dense, striate,
outer (primary) layer (Figures 1, 74, 77, 78, and 82). The
inner layer is continuous with the subbasal peg (Figures 33,
40, 49, and 50), the site of attachment of the conidium to the
sterigma of the conidiogenous cell. Whorled plasmalemmasomes,
modified invaginations of the plasma membrane, are scattered
about the periphery of the cell (Figures 1, 77, 78, 81, and
82).

Dense core vesicles (approximately 0.15 µm in diameter),
comprised of an electron-dense core and a translucent, fibrillar
outer zone, apparently arise from a granular region located
in the conidial apex (Figures 1, 74, 77, 78, 81, and 82).
These vesicles migrate throughout the conidium and become
associated with the conidial wall, possibly functioning in
secretion of the thick (1.0 µm) electron-dense fibrillar
coating that has been observed to surround fully mature conidia.
This coating, which consists of fibrils that are oriented
perpendicular to the conidial wall, is most likely mucilaginous
in nature to allow the adhesion of conidia to the host cuticle
(Figures 2, 3, 4, 6, 7, 18, 19, 22, and 25).

The proximal half of the conidium contains numerous ovoid mitochondria measuring 0.2-0.4 x 0.3-0.5 μm as well as one or two prominant (approximately 2.5 μm in diameter) double-membrane bound inclusions that are presumably autophagosomes or autophagic lysosomes (Figures 1, 64(l, m, and n), 74, 77, 78, 81, and 82). If two such inclusions are present, they apparently fuse as the conidium matures. The autophagosome(s) appears to be actively absorbing lipid bodies and discrete packets of ribosomes, which it digests in addition to endoplasmic reticula, mitochondria, and miscellaneous vesicular inclusions (Figures 1, 78, and 81). A nucleus (approximately 1.0 μm in diameter) is situated proximal (Figures 1 and 78) or more often immediately distal (Figures 81 and 82) to the autophagosome. In addition to the aforementioned inclusions, lipid bodies, various types of vesicles, and numerous ribosomes are scattered throughout the dense cytoplasm of the conidium.

Adhesion of Conidia to Infection Sites:

For initiation of infection, conidia floating on or near the water surface may either adhere to the larval epicuticle or be indiscriminately ingested with food particles. Ingested conidia may adhere firmly to the foregut and hindgut regions of the gut cuticle or pass through the gut apparently unchanged. Although conidia adhere randomly to the epicuticle or become trapped within intersegmental folds (Figures 36-48), at high concentrations (10^4- 10^6 conidia/ml) they show preferential

attachment to the anal gills and the area around the anal pore (Figures 30(a-e), 31, 32, and 35). The thin epicuticle in these areas may therefore provide a secondary site through which the fungus can infect the larva. The primary infection site is, however, the larval foregut and hindgut.

Adhesion of conidia to both the epicuticle and the gut lining appears to be via the "mucilaginous", electron-dense, fibrillar coating that encases mature conidia. This coating, which is sometimes sloughed from conidia (Figures 2, 6, and 13), provides a strong, presumably physical, bond that withstands the jerking, spasmotic movements characteristic of healthy larvae. In addition, this coating perhaps attracts bacteria that become associated with the conidium (Figures 2, 3, 4, 5, 7, 9, 31, 46, and 47).

Germination of Conidia:

Each conidium germinates via a germ tube that grows from the narrow end of the cell. This usually occurs within two hours of conidial adhesion to the host cuticle. In this apparently metabolically active cell, a third electron-dense (tertiary) wall layer (0.03 μm thick) becomes evident between the plasma membrane and the electron-translucent granular inner layer (Figures 3, 4, and 14). During germination, the primary wall layer and mucilaginous fibrillar coating fracture. The secondary wall material that is deposited around the elongating germ tube is apparently synthesized in a 0.4 μm wide collar that is located between the tertiary wall layer and the

secondary wall layer (Figures 4, 5, 7, 8, 9, 10, and 11).
The germ tube grows toward the cuticle (Figures 5, 7, 8, 9,
10, and 11) and either penetrates (Figures 12, 13, 14, 15,
16, and 17) or grows along the surface in contact with the
cuticle (Figures 37, 44, 45, 46, 47, and 48). In some instances,
the germ tube is delimited from the conidium by a septum
(Figure 22). Irregular and regularly whorled plasmalemmasomes
are found about the periphery of most conidia (Figures 4 and
18). The tertiary wall layer follows the contours of the
irregular plasmalemmasomes (Figure 4).

During germination of conidia, a number of changes occur
among the cellular inclusions. The autophagosome migrates to
the proximal end of each conidium and now contains vesicular
electron-dense material that is presumably the undigested
residue of cellular organelles (Figures 4, 5, 6, 9, 13, and 17).
During this phase, enzymes within this inclusion apparently
digest its inner membrane to form a "residual body". As
germination progresses, the vesicular contents of this
inclusion migrate to its boundary (Figures 9 and 13) or
coalesce to form a fibrous, electron-dense sphere (Figure 17)
that is visible via light microscopy (Figures 30(a-e)). The
nucleus, located distal to the residual body, usually contains
an ovoid, peripheral nucleolus (Figures 4, 11, 13, and 26).
In addition, the many scattered mitochondria present in the
cytoplasm appear to have fused to form a single elongate
mitochondrion that extends the entire length of the conidium
(Figures 4, 7, and 22). Lipid bodies (Figures 2, 3, 4, 7, 12,

and 14) and granular bodies (Figures 3, 4, 9, and 14),
measuring approximately 0.3 μm in diameter, as well as opaque
vesicles (Figures 10 and 13) and granular endoplasmic reticula
(Figures 3, 4, and 25) are located throughout both conidia and
germ tubes. In addition to the ribosomes attached to the
endoplasmic reticula, free ribosomes and polyribosomes are
uniformly distributed throughout the cytoplasm. Dense body
vacuoles which appear to originate from the residual body are
found within conidia (Figures 3, 6, 9, and 17). Microfilaments
located in the distal half of conidia are usually observed in
association with the mitochondrion (Figure 4).

   With elongation of the germ tube, conidial cytoplasm
and associated inclusions migrate from the conidium into the
germ tube. Mitochondria moving into the germ tube appear to
bud from the distal end of the elongate mitochondrion (Figures
4, 7, 11, and 12).

Cuticle Penetration:

   Host response to penetrant hypha is often evident as
melanization of host tissues. Such a response is recognized
by a darkening of the tissue adjacent to the penetration site
and/or around the elongating hypha(e) (Figures 12, 15, 16,
17, 20, and 21). The melanins appear to be deposited
concentrically around the penetrant hyphae and form a barrier
that physically contains the fungus. However, the hyphae
usually rupture the barrier to grow throughout the host
(Figure 23). In most instances, melanization is accompanied

by apparent hardening (sclerotization) of host tissue; a condition which may cause lateral deflection of hyphae for short distances (Figure 22). Hyphae within the larval hemocoel are sometimes encapsulated within a substance that is presumably humoral in origin.

At the point of contact between the germ tube tip and the host cuticle there is apparent corrosion of the cuticle (Figures 9, 10, 11, and 41). Such corrosion is probably mediated via a dense, amorphous material that is deposited in the cavity between the germ tube and the cuticle. This amorphous material appears to be secreted from the germ tube tip and may be the product of the histolytic breakdown of host tissue or perhaps play some role in anchorage of the conidium. Remnants of the mucilaginous coat sloughed from the conidium often persist about the growing germ tube (Figures 7, 8, 9, 10, 11, and 22).

Within six hours following conidial adhesion, the germ tube (penetrant hypha) has pierced the larval cuticle. At this stage, the penetrant hyphae, which retains its secondary wall layer (Figures 13, 14, 15, and 22), is surrounded at the point of entry by a collar of host tissue (Figures 13, 14, 15, 16, 17, 22, 23, 26, 41, and 42). Numerous bacteria are usually present in the area around the entry site. Once firmly anchored to the larva by the penetrant hypha, the conidium may break its lateral adhesion to the cuticle (Figures 13, 17, and 22). After the penetrant hypha has grown to a length

of 3-6 μm, a septum is usually formed near its growing tip.
The septal wall tapers from the hyphal wall towards a central
pore, which is sometimes blocked by a septal plug. Woronin
bodies (Woronin, 1866) are usually found in association with
the septum in the vicinity of the pore (Figures 26-29). With
continued growth, a spherical to ovoid hyphal cell forms at
the tip of the penetrant hypha (Figures 23, 24, 25, 26, and
30(b, c, and d)). This usually occurs within eight hours
after infection. A single vegetative hypha typically arises
from the hyphal cell (Figures 26 and 30(e)). Utilization of
host tissues adjacent to the vegetative hypha is evidenced by
a zone devoid of tissue around the hypha and hyphal cell
(Figures 25 and 26).

Conidial organelles undergo no noticeable changes during
the infective process other than migrating into the penetrant
hypha. With hyphal growth all organelles appear to increase
in number and migrate through the penetrant hypha, the hyphal
cell, and finally into the vegetative hypha(e).

Hyphal Proliferation and Epicuticular Rupture:

The vegetative hypha that arises from the hyphal cell is
typically 1.0 μm in diameter and has a cell wall approximately
0.08 μm thick. Proliferation of branches and hyphal buds from
the initial vegetative hypha result in the rapid spread of the
fungus throughout the host hemocoel. Such proliferation is
first apparent in the anal gills about the time of larval
death, approximately 24 hours following conidial adhesion.

Within 48-60 hours, hyphae fill the abdomen, thorax, and head
(Figure 55). Once the hemocoel is filled with hyphae,
epicuticular rupture occurs first in the pliable cuticle
between segments, then in the epicuticle of the anal gills,
the abdomen, and finally the thorax.

Conidiogenesis:

Within 24 hours of epicuticular rupture, the formation
of singly-borne lateral or terminal conidia is initiated on
conidiogenous hyphae that are 32-48 μm long. In vitro time-
lapse photomicrographs (Figures 63(a-p)) show that
conidiogenesis in C. clavosporus takes approximately ten
hours to complete. A dense layer of conidia then envelopes all
but the head and siphon of the larva (Figures 56-59). Light
observations of sectioned larvae have revealed that conidia
are also formed within the gut lumen.

Conidiogenesis is first evident when the lateral or
terminal conidiogenous cells are initiated as hyphal evaginations
from the emergent hyphae. Such evaginations swell into
spherical to ovoid conidiogenous cells that measure 2-3 x
3-6 μm (Figures 63(a-h), 64(a-g), and 65-68). The distal
portion of the conidiogenous cells give rise to typically one,
but sometimes two sterigmata (0.1 μm in diameter by 4.0 μm
long) once the cell has been delimited by a septum (Figures
65, 66, 67, 68, 78, and 80). The entire conidiogenous cells
are surrounded by the bilaminar wall that consists of an inner
translucent layer (0.08 μm thick) and a thin outer electron-

dense layer (Figures 65, 66, 69, and 70). The conidial initial grows from the distal apex of the flask-shaped conidiogenous cell. The thick electron-translucent, granular wall of the conidial initial is apparently synthesized and deposited in the region of the sterigma immediately proximal to the conidiogenous locus. As the cytoplasm of the conidiogenous cell swells at the conidiogenous locus, the bilaminar wall of the conidiogenous cell is fractured by the developing conidial initial. The wall remnants of the conidiogenous cell form a collarette at the conidiogenous locus (Figures 69, 70, 73, and 74) that sometimes persists about the conidium (Figures 76, 77, and 79). As the conidial initial develops, a thin electron-dense striate wall layer is deposited outside the electron-translucent layer (Figures 70, 73, 74, 77, 78, 81, and 82). Upon reaching maturity, the conidium is delimited from the cell by a septum proximal to the subbasal peg. An abscission zone is formed between the septum and the subbasal peg and allows the conidium to be easily dislodged from the conidiogenous cell (Figures 74, 77, and 78).

The number and complexity of organelles within the conidium increases as the cell matures. The conidial initial contains the elongate mitochondria, ribosomes, and lipid bodies within its dense cytoplasm. In addition, whorled plasmalemmasomes are present around the periphery of the cell (Figures 69, 70 and 73). The immature conidium has a number of developing inclusions along with those previously described. These include rough and smooth endoplasmic reticula, as well as numerous

vesicles that have yet to mature. Also, a multivesicular complex and dense body vacuoles are present and may be precursors of the autophagosome(s) found in the mature conidium (Figure 73). These organelles migrate across the neck of the conidiogenous cell into the developing conidium prior to the formation of the septum.

Figure 1. Transmission electron micrograph of a mature
           conidium showing the internal arrangement of
           organelles. Note the centrally located double-
           membrane bound autophagosome. 34,200x. A,
           autophagosome; dcv, dense core vesicle; gr,
           granular region; L, lipid body; M,
           mitochondrion; N, nucleus; pwl, primary wall
           layer; sbp, subbasal peg; swl, secondary wall
           layer; wps, whorled plasmalemmasome.

gr

dcv

L

A

M

pwl→

swl→

N

wps

sbp

1

0.5 μ
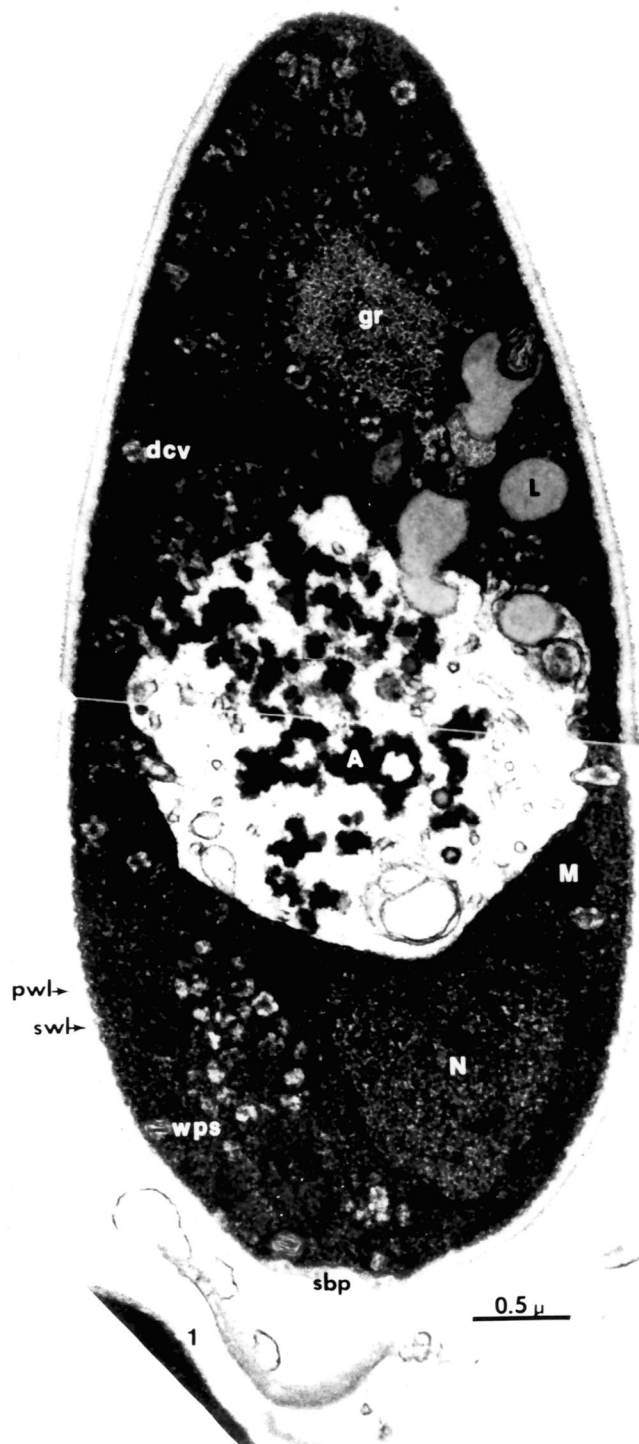
Figure 2.   Longitudinal section of a conidium adhering to
            the foregut cuticle of the larva. 24,200x.
            GC, gut cuticle; L, lipid body; Lu, lumen of
            gut.

Figure 3.   Diagonal section of a conidium adhering to the
            foregut cuticle. Note outer "mucilaginous"
            coating of the conidium. 36,000x. b, bacterium;
            dbv, dense body vacuole; gb, granular body;
            GC, gut cuticle; L, lipid body; M, mitochondrion;
            mc, mucilaginous coat; pm, plasma membrane; RER,
            rough endoplasmic reticulum; swl, secondary wall
            layer; twl, tertiary wall layer.

Lu

GC

L

0.5 µ

2

mc→

pm→
tw→
sw→

b

M

db→

G

RER

L

0.5 µ

3
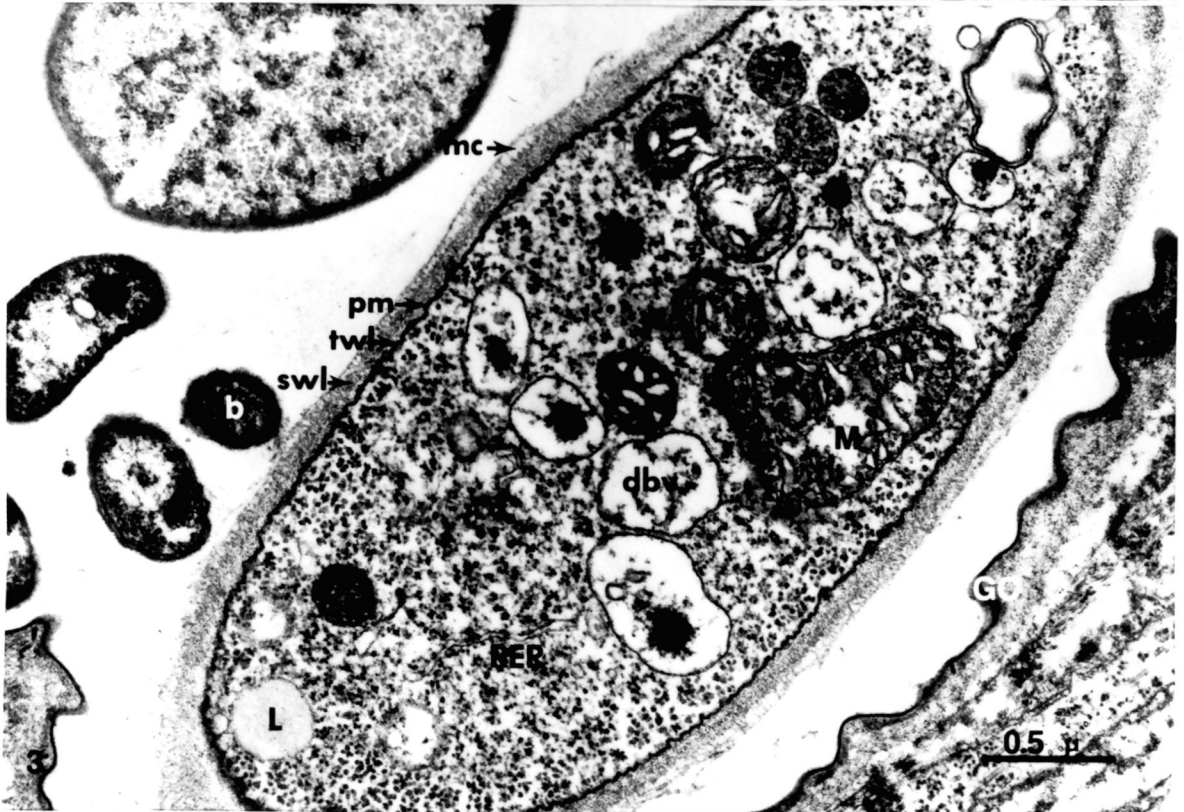
Figure 4.   Longitudinal section of a germinating conidium
             showing the internal arrangement of organelles.
             Note the fracture of the mucilaginous coat and
             primary wall layer by the emerging germ tube.
             The white arrow denotes the synthesis site of
             secondary wall material that is deposited around
             the emerging germ tube.   27,000x.   b, bacterium;
             f, wall fracture; gb, granular body; GT, germ
             tube; M, mitochondrion; mc, mucilaginous coat;
             mf, microfilament; N, nucleus; No, nucleolus;
             pls, irregular plasmalemmasome; pm, plasma
             membrane; pwl, primary wall layer; RB, residual
             body; RER, rough endoplasmic reticulum; swl,
             secondary wall layer; twl, tertiary wall layer;
             wps, whorled plasmalemmasome.

GT

f

b

wps

M

mf

mc
pwl
swl
twl
pm

RER

N

No

pls

PB

0.5μ

4
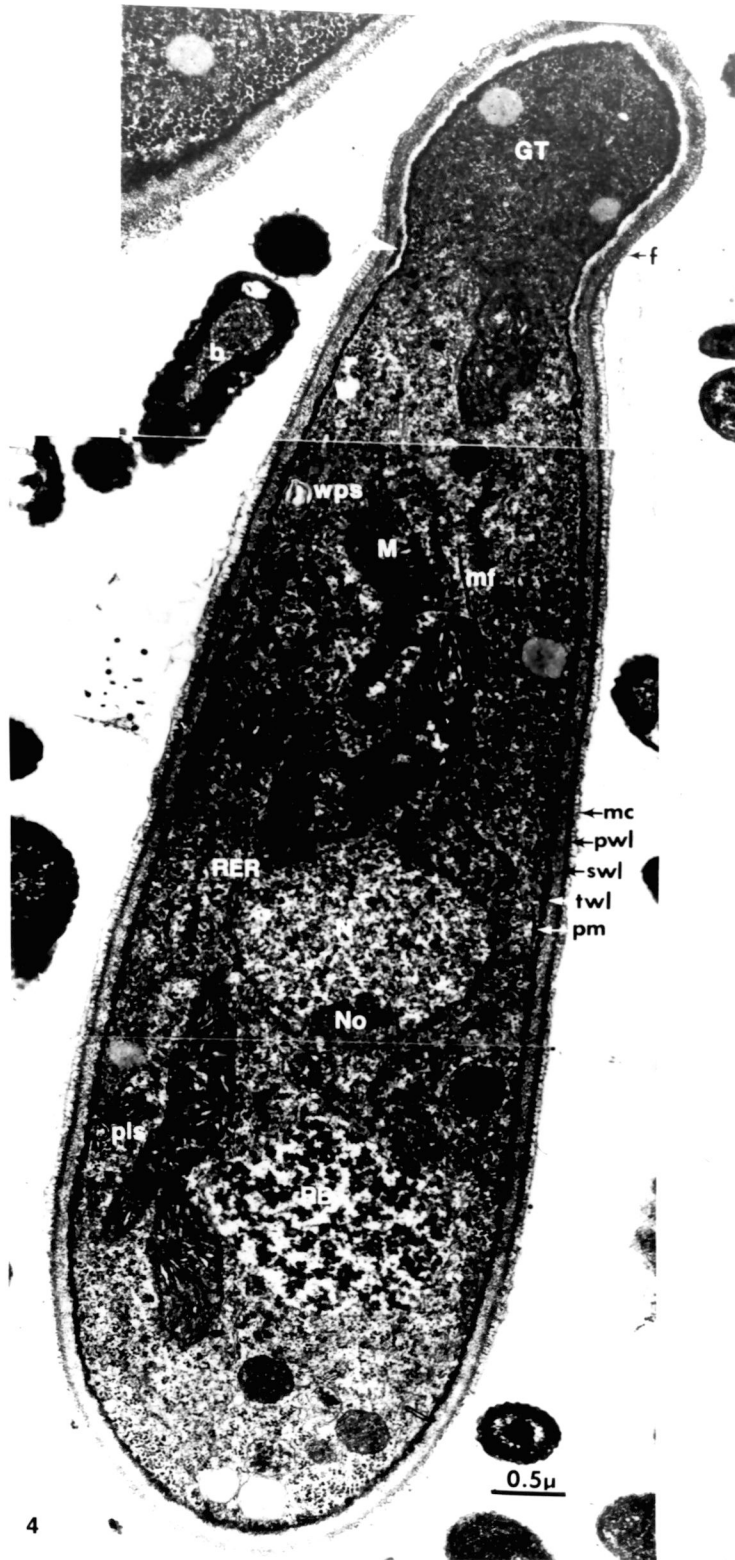
Figure 5.　　Germinating conidium adhering to the hindgut
　　　　　　　cuticle. The black arrow denotes the site of
　　　　　　　secondary wall synthesis and deposition. 12,640x.
　　　　　　　b, bacterium; GC, gut cuticle; GT, germ tube;
　　　　　　　Lu, lumen of gut; N, nucleus; RB, residual body.

Figure 6.　　Cross-section of a conidium adhering to the
　　　　　　　hindgut cuticle. The vesicular contents of the
　　　　　　　residual body are presumably the undigestible
　　　　　　　residue of cellular organelles. 15,360x. dbv,
　　　　　　　dense body vacuole; M, mitochondrion, mc,
　　　　　　　mucilaginous coat; RB, residual body.

Figure 7.　　Diagonal section of a germinating conidium
　　　　　　　adhering to the hindgut cuticle. Note fracture
　　　　　　　of the primary wall layer. 16,320x. f, wall
　　　　　　　fracture; l, lipid body; M, mitochondrion; mc,
　　　　　　　mucilaginous coat.

Figure 8.　　Germ tube approaching the gut cuticle. Note
　　　　　　　the site of wall synthesis. 34,200x. f, wall
　　　　　　　fracture; GC, gut cuticle; R, ribosomes.

Lu

GC

N

GT

b

1.0 μ

RB

M

dbv

mc

6

1.0 μ

mc

M

f

f

L

7

1.0 μ

R

f

f

GC

8

0.5 μ

29
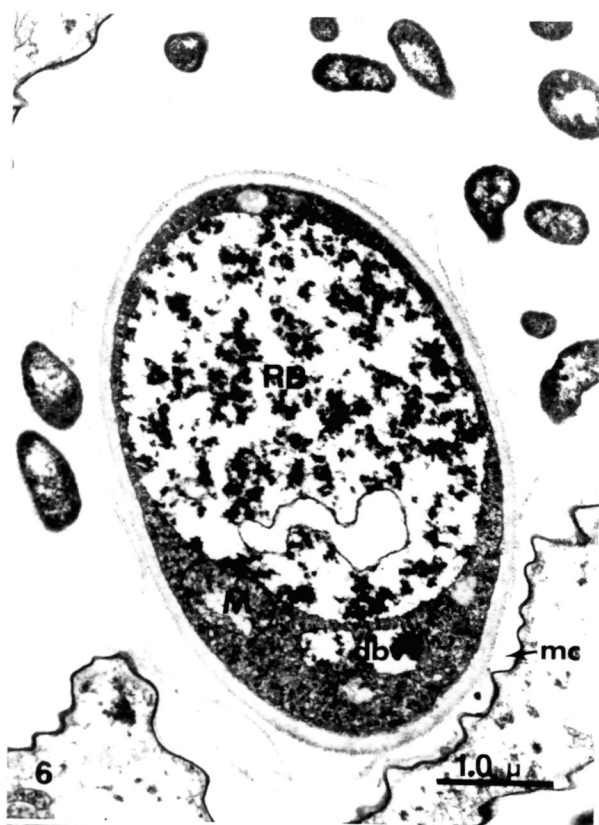
Figure 9.   Longitudinal section of a germinating conidium.
             Note the amorphous material between the germ
             tube and gut cuticle. 15,010x. Am, amorphous
             material; dbv, dense body vacuole; gb, granular
             body; GC, gut cuticle; GT, germ tube; RB,
             residual body; SER, smooth endoplasmic reticulum.

Figure 10.   Germ tube approaching contact with the foregut
             cuticle. Note the cuticular cavity beneath the
             germ tube. 27,000x. Am, amorphous material;
             Ca, cavity; GT, germ tube; M, mitochondrion;
             ov, opaque vesicle; SER, smooth endoplasmic
             reticulum.

Figure 11.   An early stage of cuticular penetration by the
             germ tube. 16,500x. Ca, cavity; f, wall fracture;
             N, nucleus; No, nucleolus.

9

RB

dbv

GC

Am

1.0 µ

GT

M

SER

ov

Am

Ca

10

0.5 µ

No

f

f

Ca

11

1.0 µ

31
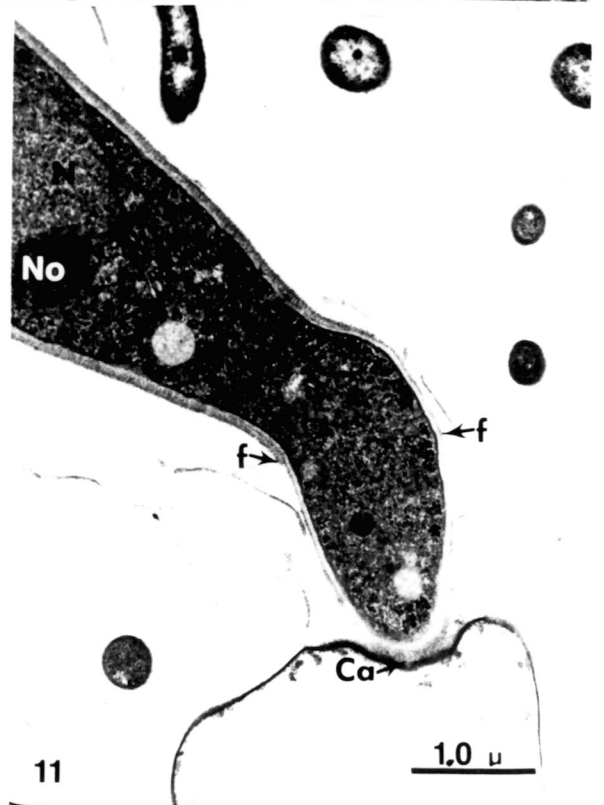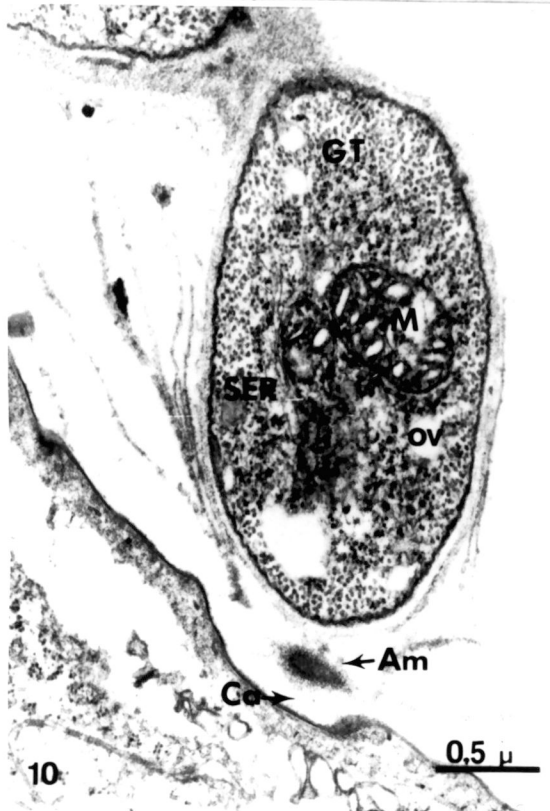
Figure 12.   Early stage of cuticular penetration. Germ
tube (penetrant hypha) abrasion of host tissue
triggers melanization. 15,600x. GC, gut
cuticle; L, lipid body; M, mitochondrion; Me,
melanization; mvc, multivesicular complex.

Figure 13.   Penetration of hindgut cuticle via penetrant
hypha. Conidial adherence to the cuticle has
been broken. 15,120x. C, collar; N, nucleus;
No, nucleolus; ov, opaque vesicle; Ph, penetrant
hypha; pls, irregular plasmalemmasome; RB,
residual body.

M

L

Me

GC

12

10

RB

pls

ov

C→

Ph

1.0 μ

13

33
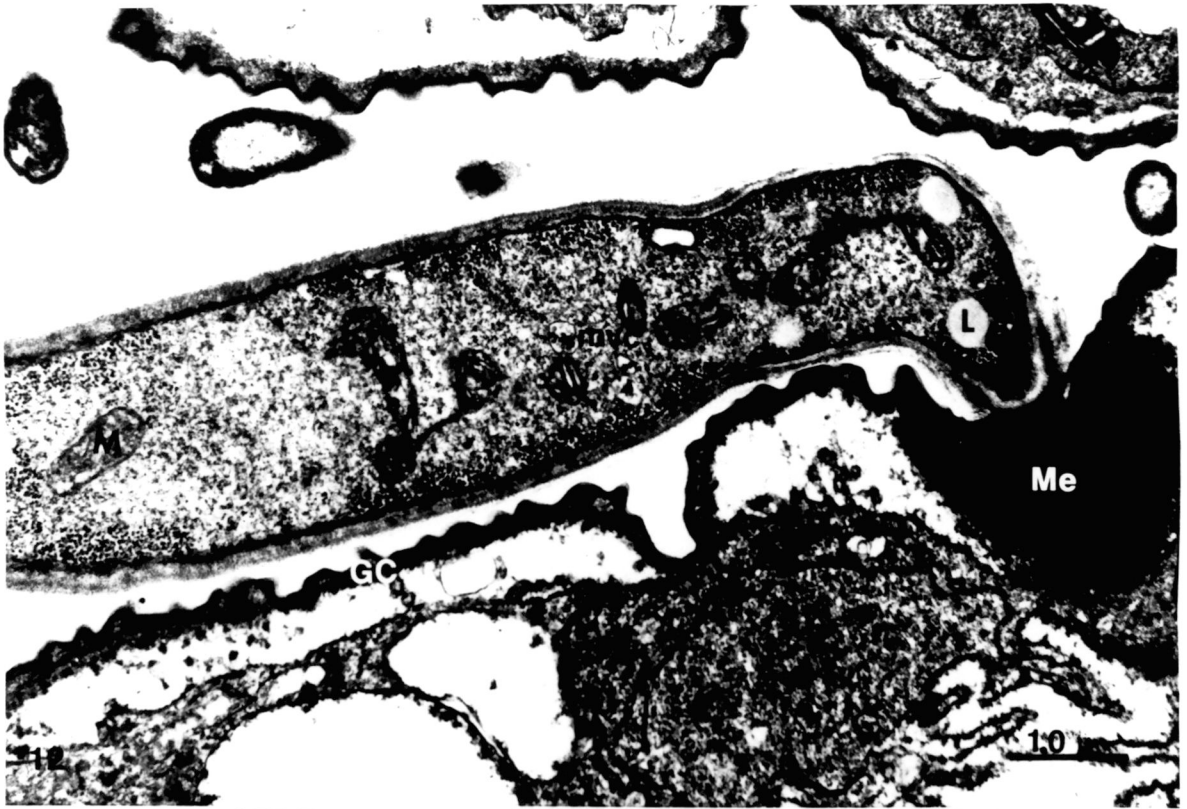
Figure 14. Penetrant hypha piercing the foregut cuticle.
Note the tertiary wall layer and secondary wall
layer surrounding the penetrant hypha. 72,600x.
C, collar; gb, granular body; GC, gut cuticle;
L, lipid body; M, mitochondrion; pm, plasma
membrane; R, ribosomes; SER, smooth endoplasmic
reticulum; swl, secondary wall layer; twl,
tertiary wall layer.

Figure 15. Penetrant hypha piercing the hindgut cuticle.
Note collar of host tissue around penetration
site. 25,600x. C, collar; L, lipid body;
Me, melanization.

Figure 16. Penetrant hypha piercing foregut cuticle.
32,400x. b, bacterium; M, mitochondrion.

14

L   R   C

SER   pm

fwl

iwl

GC

0.2 μ

15   C   L

0.5 μ

16   b   0.5

35

Figure 17.   Firm anchorage of conidium via the penetrant
              hypha. Note fibrous sphere in residual body.
              12,600x. b, bacterium; C, collar; dbv, dense
              body vacuole; fs, fibrous sphere; N, nucleus;
              Ph, penetrant hypha; RB, residual body.

Figure 18.   Cross-section of conidial apex and germ tube.
              27,000x. Cm, conidium; GT, germ tube; M,
              mitochondrion; mc, mucilaginous coat; pls,
              irregular plasmalemmasome.

Figure 19.   Cross-section of conidial apex. Note primary,
              secondary, and tertiary wall layers. 27,000x.
              L, lipid body; pwl, primary wall layer; R,
              ribosomes; swl, secondary wall layer; twl,
              tertiary wall layer.

17

18

19
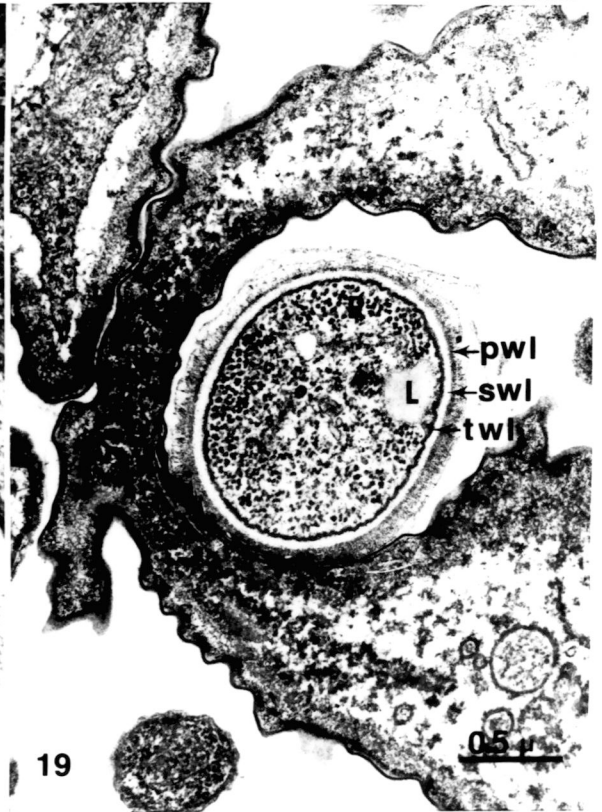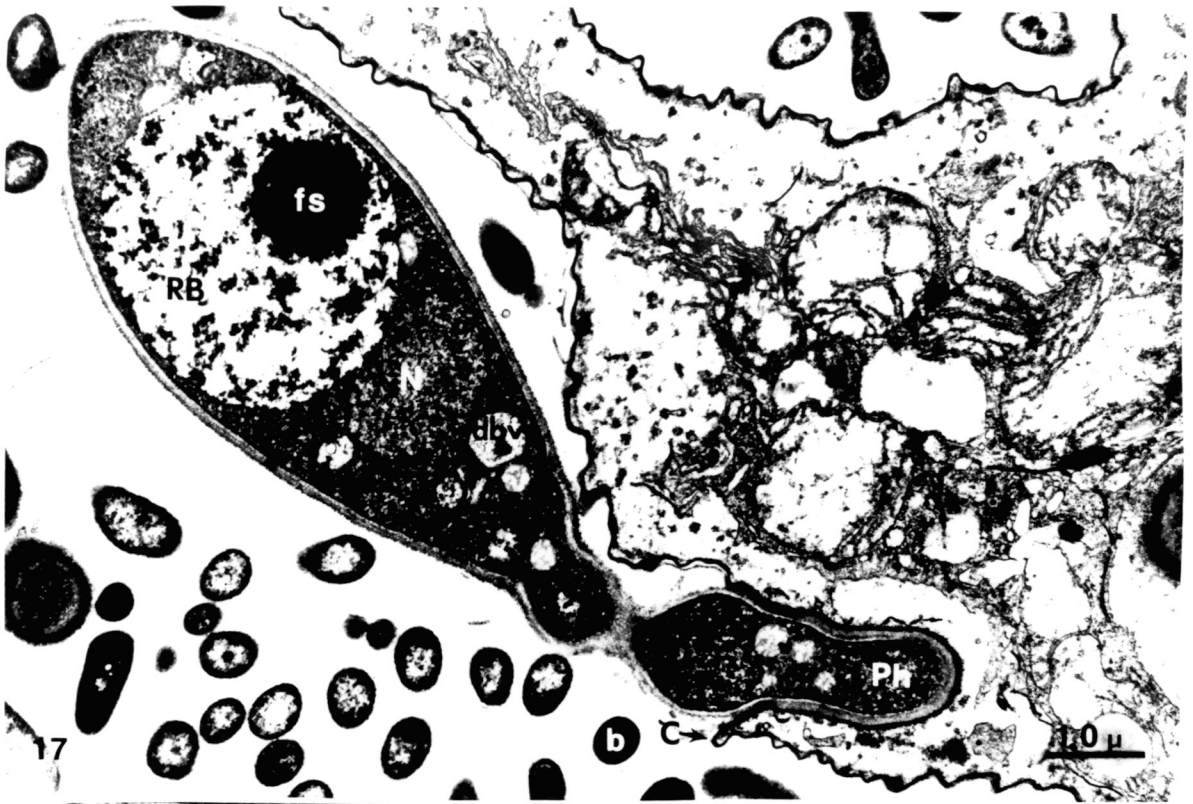
Figure 20. Melanization of host tissue in response to
            hyphal penetration. 27,000x. H, hypha;
            Me, melanization.

Figure 21. Cross-section of hypha in host tissue. Note
            concentric zones of melanization elicited in
            response to the growing hypha. 14,400x.
            H, hypha; Lu, lumen of gut; Me, melanization.

Figure 22. Deflection of penetrant hypha parallel to the
            gut lumen by sclerotized tissue associated with
            melanization. Note septum between the conidium
            and germ tube. 15,800x. C, collar; L, lipid
            body; M, mitochondrion; mc, mucilaginous coat;
            Me, melanization; RB, residual body; se, septum.

21

0.5 μ

1.0 μ

Me

Me

Lu

L

M

RB

C

mc

Me

22

1.0 μ
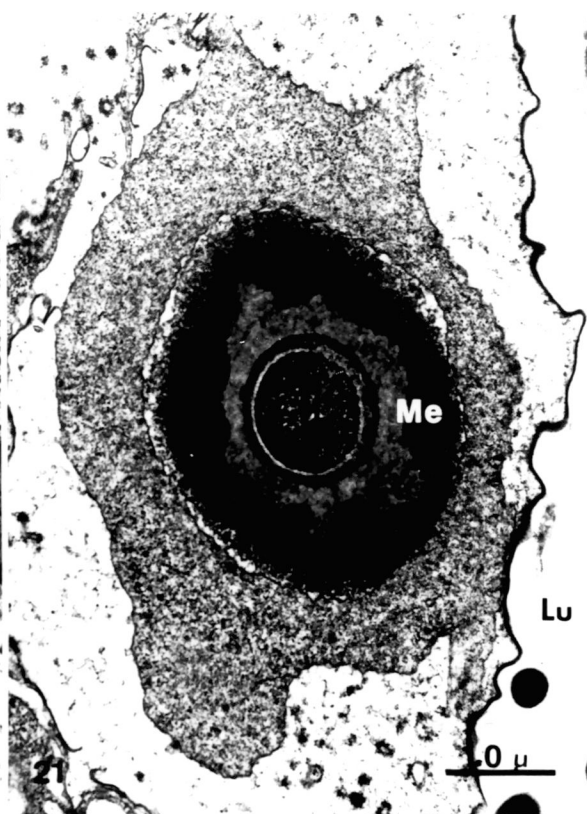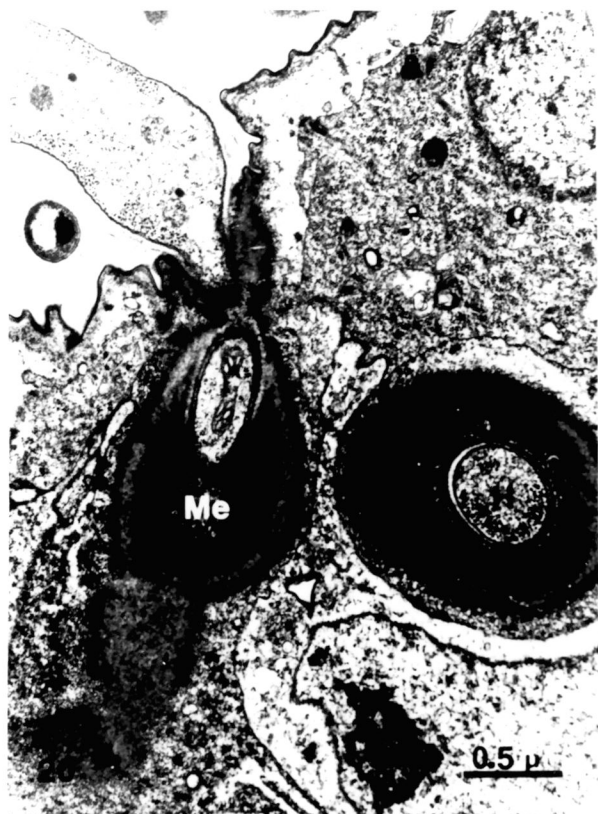
Figure 23.   Formation of hyphal cell proximal to septum.
             Note that the cell has grown through the
             melanized tissue. 9,240x. C, collar; dbv,
             dense body vacuole; HC, hyphal cell; Lu,
             lumen of gut; N, nucleus; se, septum.

Figure 24.   Lateral growth of vegetative hypha from the
             penetrant hypha. Black arrows denote fracture
             of penetrant hypha wall. 15,800x. HC, hyphal
             cell; L, lipid body; Lu, lumen of gut; Ph,
             penetrant hypha; Pl, phospholipid body; vh,
             vegetative hypha.

Figure 24

Labels visible on upper micrograph: C, Lu

Labels visible on lower micrograph: Ph, Lu, Pl, HC, L, Vh

Scale bars: 1.0 μ

24
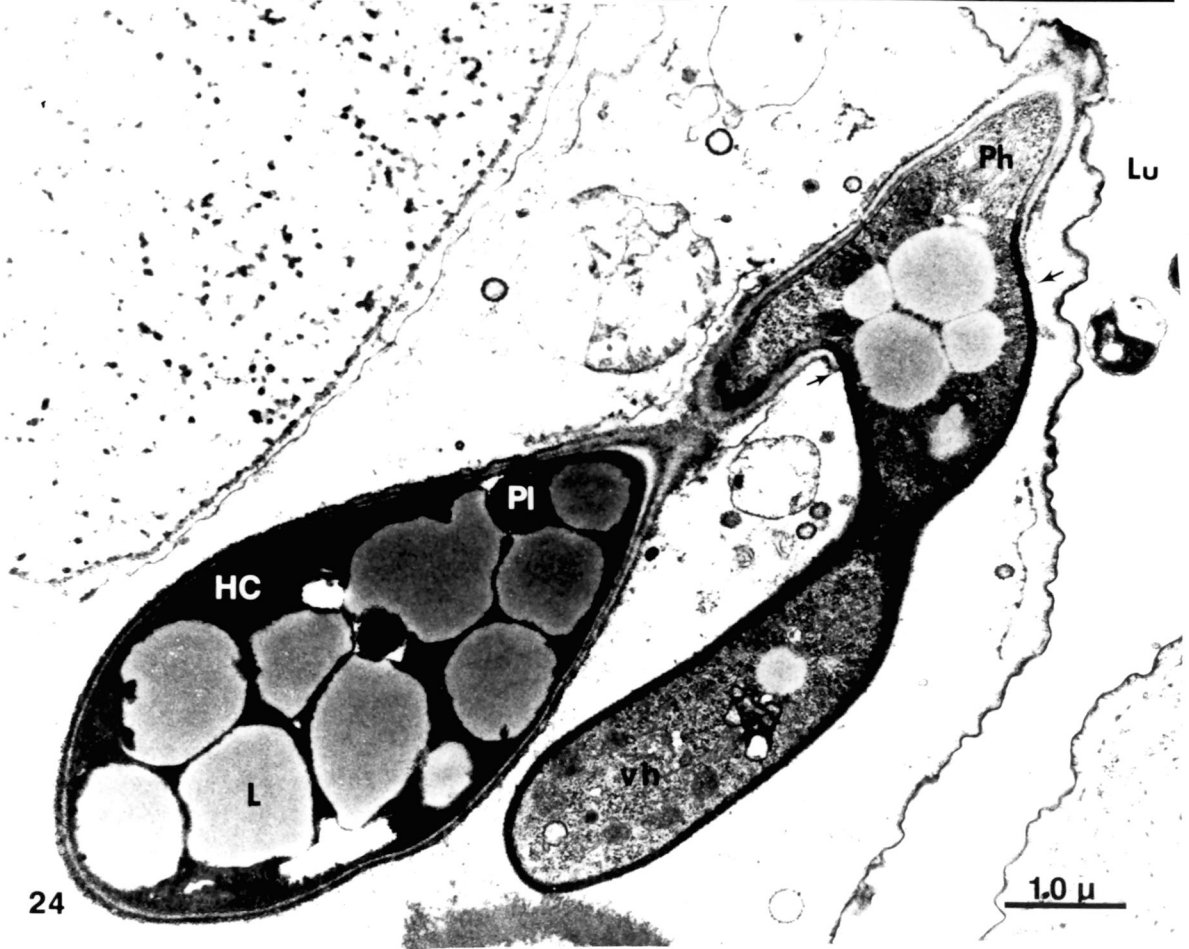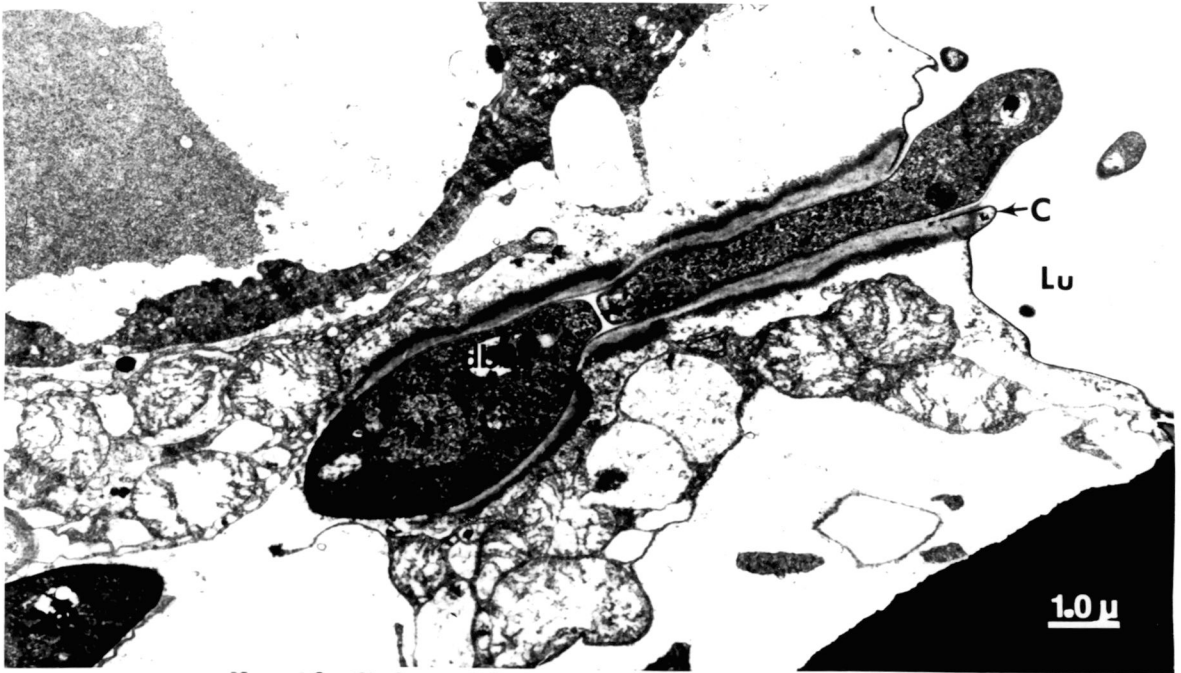
Figure 25.   Humoral encapsulation of penetrant hypha and
             hyphal cell. 27,000x. b, bacterium; HC,
             hyphal cell; he, humoral encapsulation; M,
             mitochondrion; mc, mucilaginous coat; N,
             nucleus; Ph, penetrant hypha; RER, rough
             endoplasmic reticulum.

RER

←mc

b

M

Ph

he

HC

0.5 μ

Figure 26. Transmission electron micrograph showing a
            vegetative hypha growing from the proximal pole
            of the hyphal cell. Note Woronin bodies
            associated with the septal pore. 13,200x.
            C, collar; GC, gut cuticle; H, hypha; HC,
            hyphal cell; Lu, lumen of gut; N, nucleus; No,
            nucleolus; Ph, penetrant hypha; RB, residual
            body; sp, septal pore; vh, vegetative hypha;
            W, Woronin body.

26
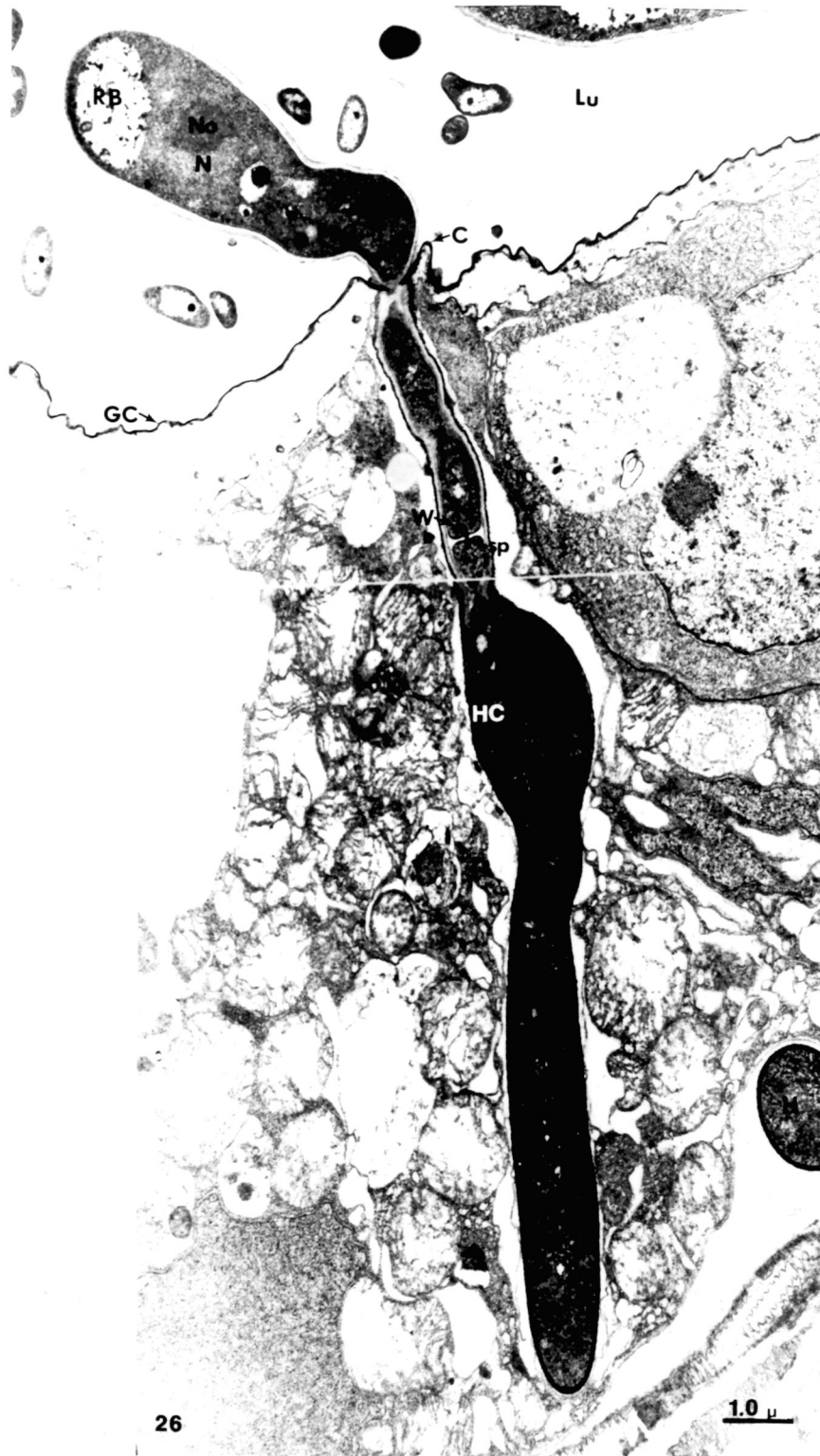
Figure 27. Hyphal septum with associated Woronin bodies.
            36,900x. sp, septal pore; W, Woronin body.

Figures 28-29. Central pore of the septum blocked by
            an electron-dense septal plug. 18,700x and
            9,600x, respectively. spl, septal plug;
            W, Woronin body.

1.0 μ

28   ←W
      ←spl
      1.0 μ

29   W→
      ←spl
      1.0 μ
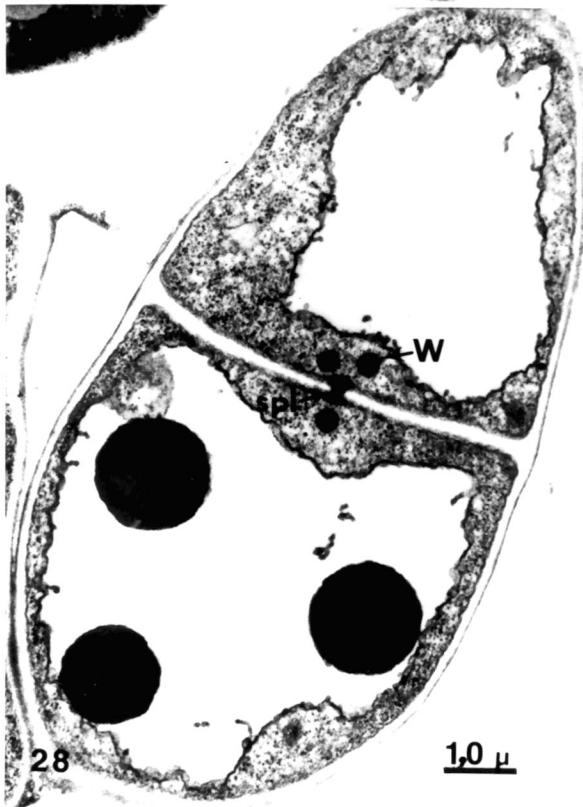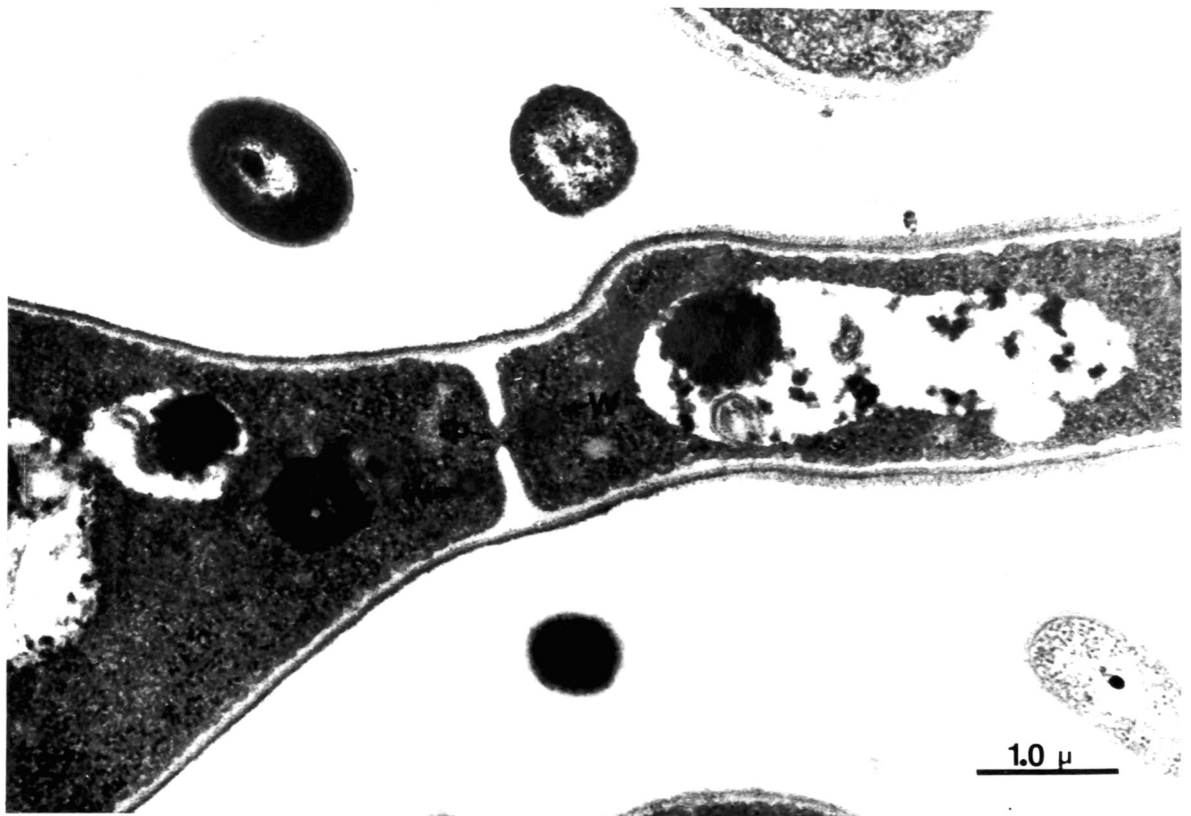
Figures 30(a-e).   Light micrographs utilizing Nomarski
                   interference contrast optics to show the
                   adherence of conidia to and subsequent
                   penetration of the anal gill epicuticle.
                   1,250x. Ep, epicuticle; GT, germ tube;
                   HC, hyphal cell; Ph, penetrant hypha;
                   RB, residual body; vh, vegetative hypha.

Figures 31-32.   Scanning electron micrographs showing the
                   adherence of conidia to the epicuticle of
                   the anal gill. 2,057x and 5,320x,
                   respectively. b, bacterium; Cm, conidium;
                   Ep, epicuticle; GT, germ tube.

30a
RB→
GT→
Ph→
HC→
Ep→
vh→

100 µ

b

e

Ep

31

5.0 µ

Cm

G

2.0 µ

49
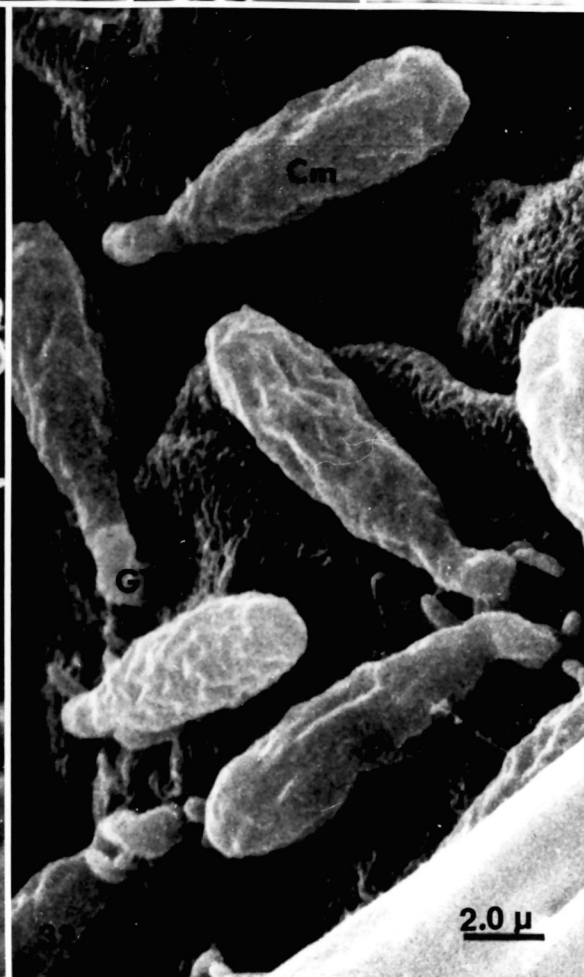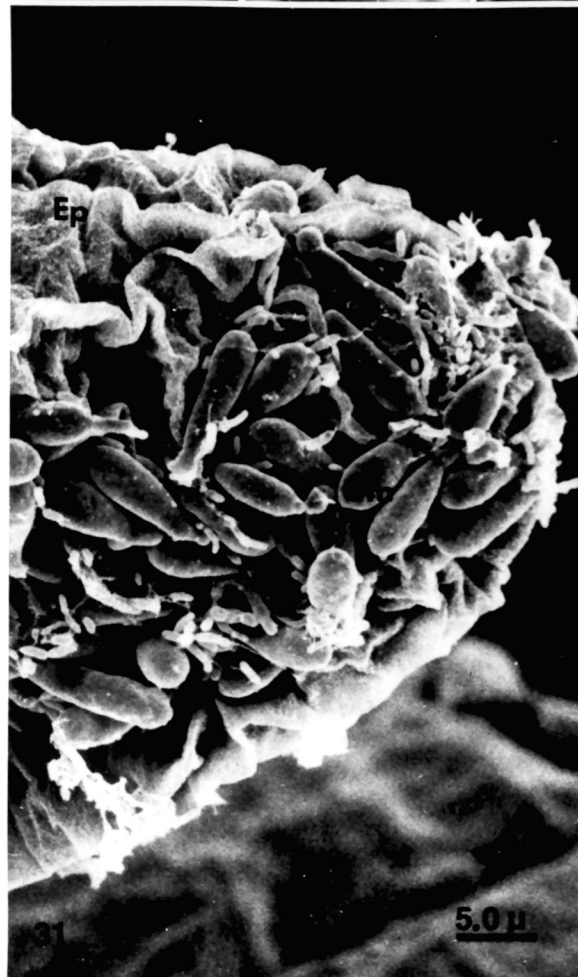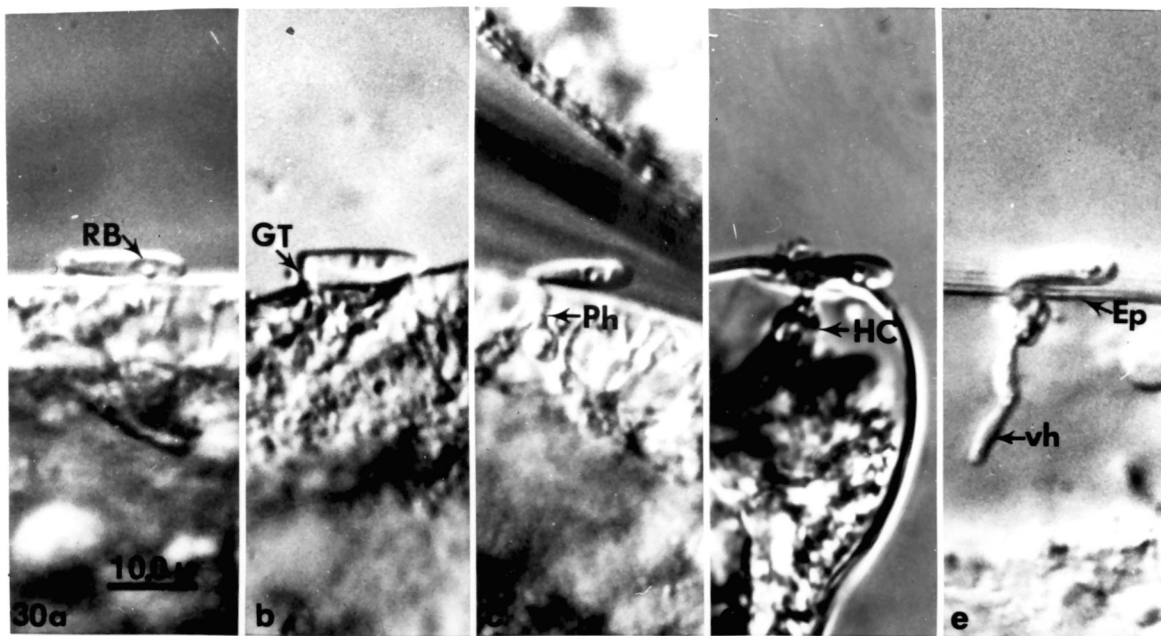
Figures 33-34. Germinating conidia attached to the larval
                siphon. Note dense bacterial flora associated
                with the conidial germ tubes. 4,875x and 975x,
                respectively. b, bacterium; Ep, epicuticle;
                sbp, subbasal peg.

Figure 35. Conidia attached to the lip around the anal
            pore. 2,058x. Ap, anal pore; Cm, conidium.

Figure 36. Conidia adhering to and trapped within the folds
            of the larval epicuticle. 2,548x.

b

cbp

2.0 µ

10.0 µ

35

Ap

Cm

5.0 µ

5.0 µ

51

Figure 37.   Conidium trapped within epicuticular fold.
             5,740x. Cm, conidium.

Figures 38-39.   Conidial germ tube in contact with epicuticle.
             Note large numbers of bacteria associated with
             the germ tube at the site of epicuticular contact.
             8,260x and 8,820x, respectively. b, bacterium;
             Ep, epicuticle; GT, germ tube.

Figure 40.   Germinating conidium that has presumably pierced
             the host epicuticle. Note subbasal peg at distal
             tip of the conidium. b, bacterium; sbp, subbasal
             peg.
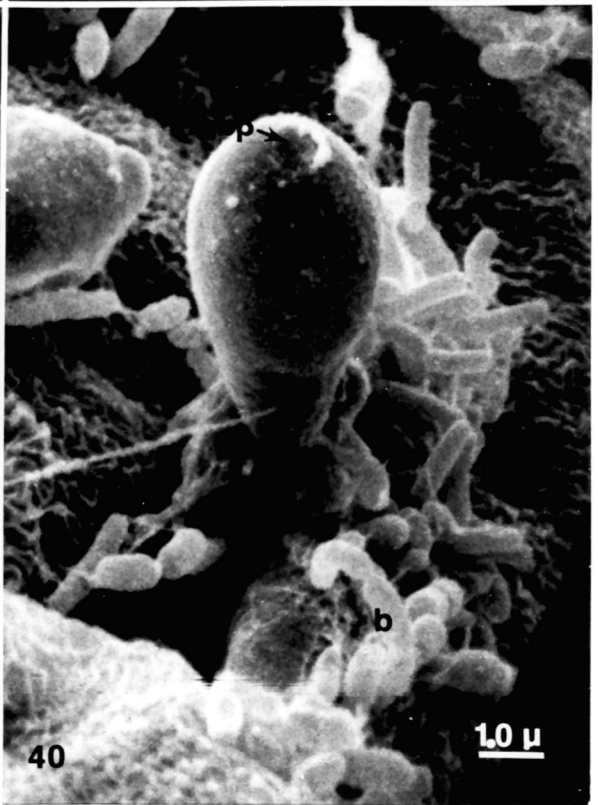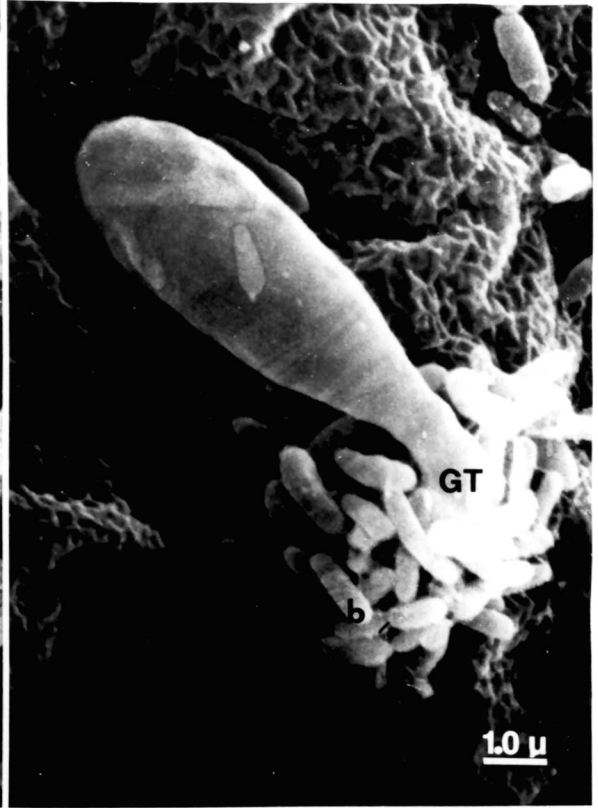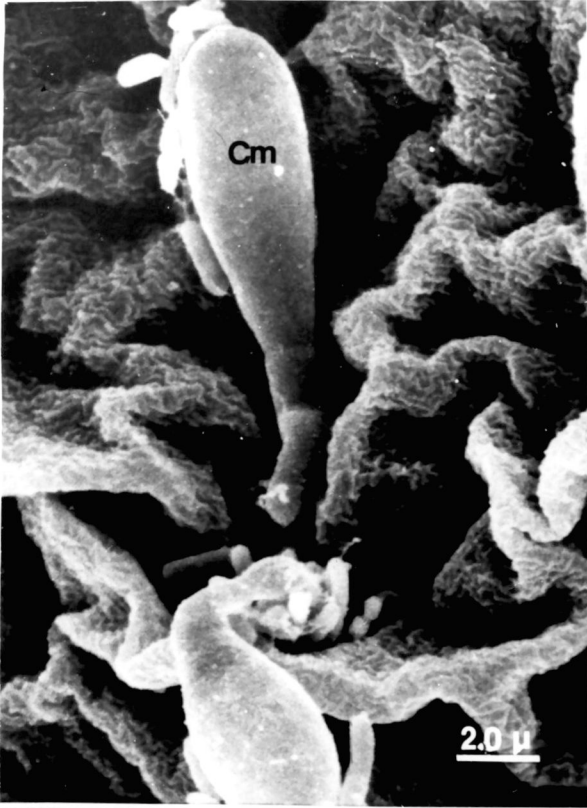
Figure 41. Germinating conidium that has successfully

accomplished penetration of the anal gill

epicuticle. Note the cavity between collar

and germ tube. 9,940x. C, collar; Ca, cavity;

Cm, conidium; GT, germ tube.

Figures 42-43. Penetration of anal gill epicuticle via

conidial germ tubes. 7,560x and 8,960x,

respectively. C, collar; GT, germ tube.

41

Cm

C

GT

Ca

1.0 μ

42

C

GT

2.0 μ

43

GT

1.0 μ
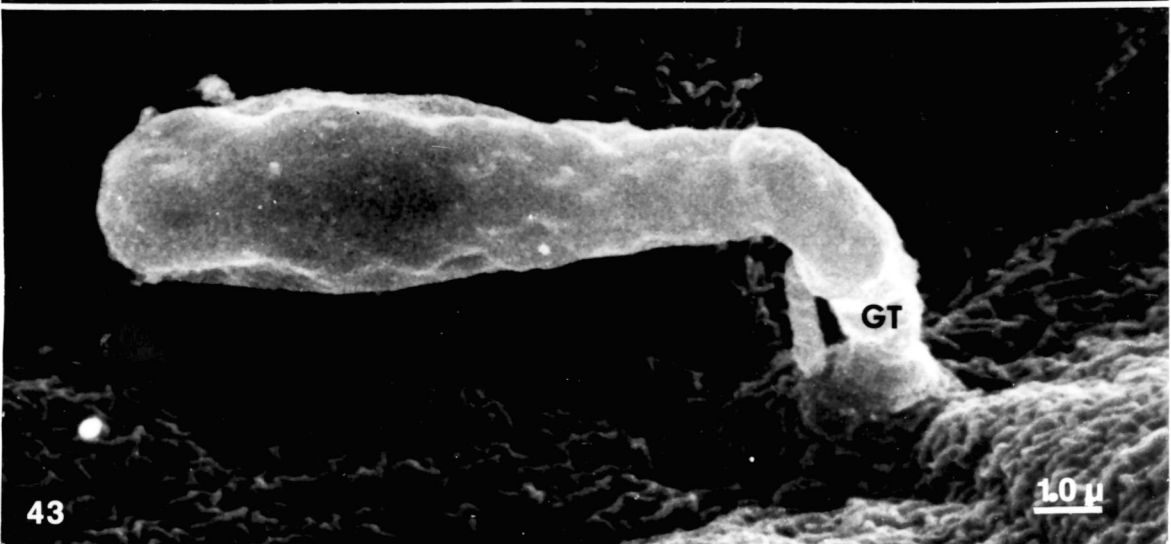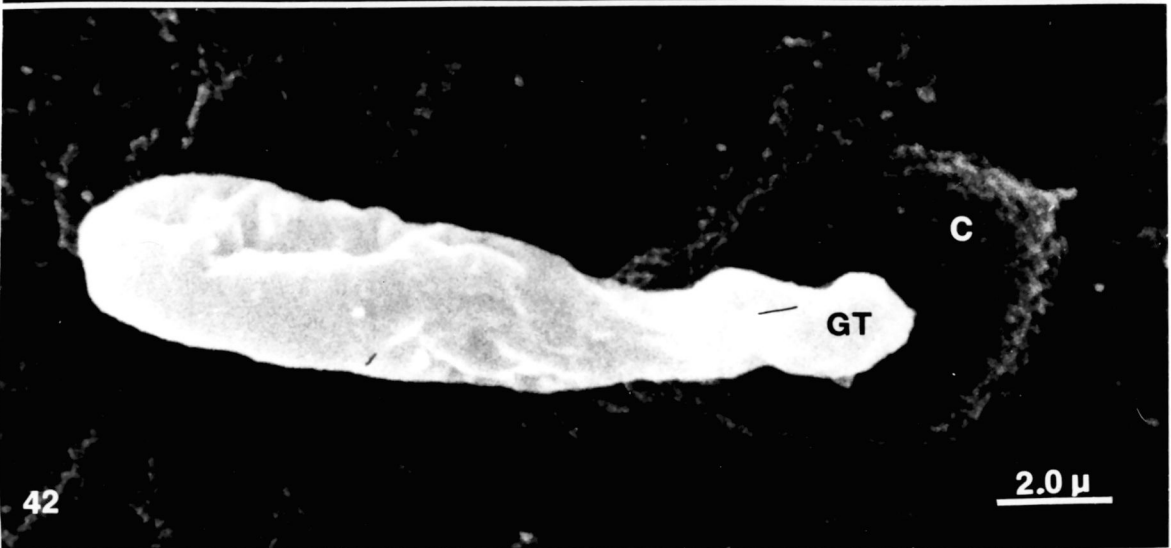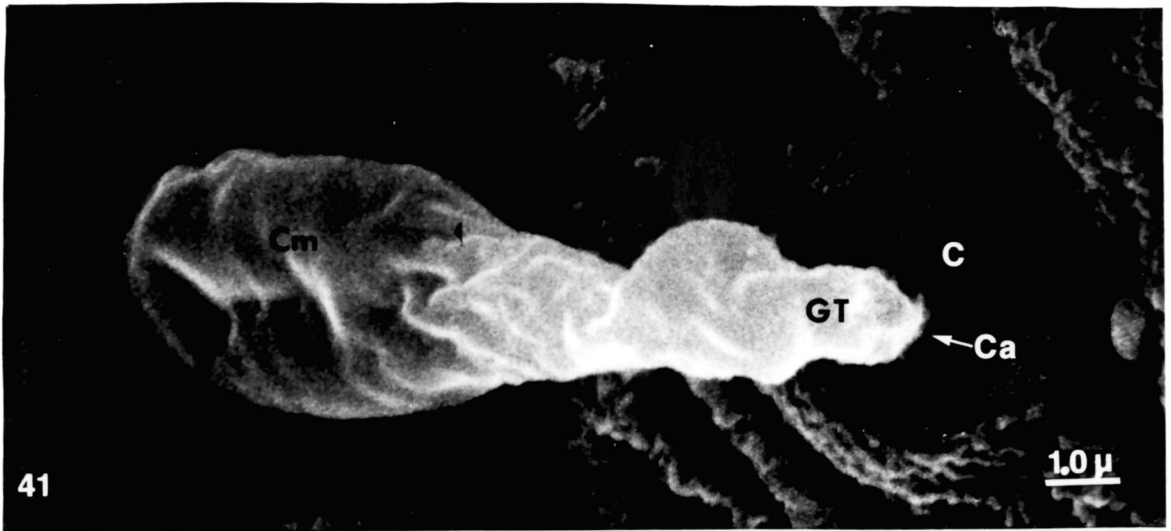
Figures 44-45.　　Conidia germinating on epicuticle of the
　　　　　　　　　　abdomen.　11,760x and 6,020x, respectively.
　　　　　　　　　　Cm, conidium; Ep, epicuticle; GT, germ tube.

Figures 46-48.　　Conidia adhering to epicuticle of the head.
　　　　　　　　　　Note the germ tube cannot pierce this smooth,
　　　　　　　　　　thick epicuticle.　4,900x, 6,020x, and 7,420x,
　　　　　　　　　　respectively.　b, bacterium; Cm, conidium;
　　　　　　　　　　Ep, epicuticle; GT, germ tube.

44

GT

45

GT

2.0 μ

46

Ep

2.0 μ

47

Cm

2.0 μ

48

b

Ep

GT

2.0 μ
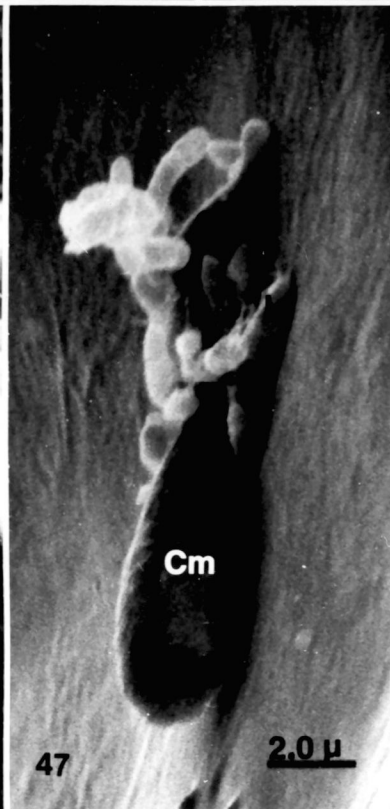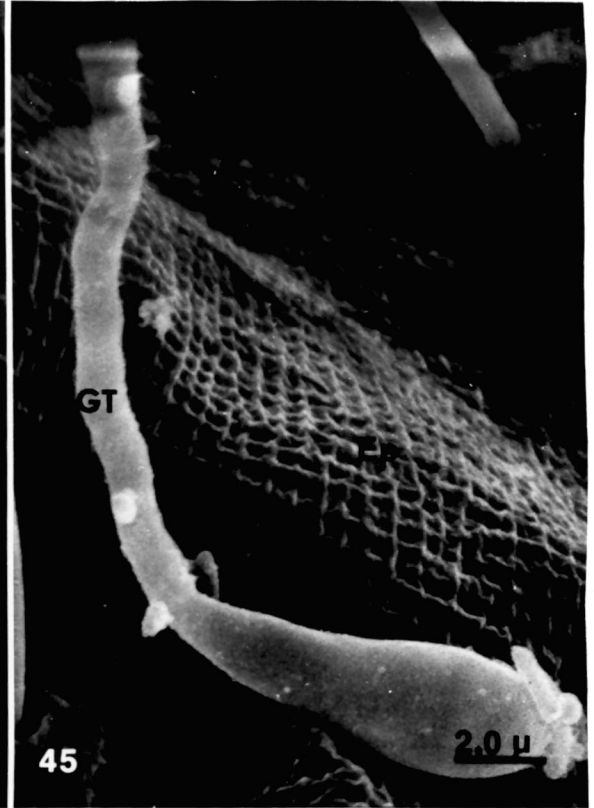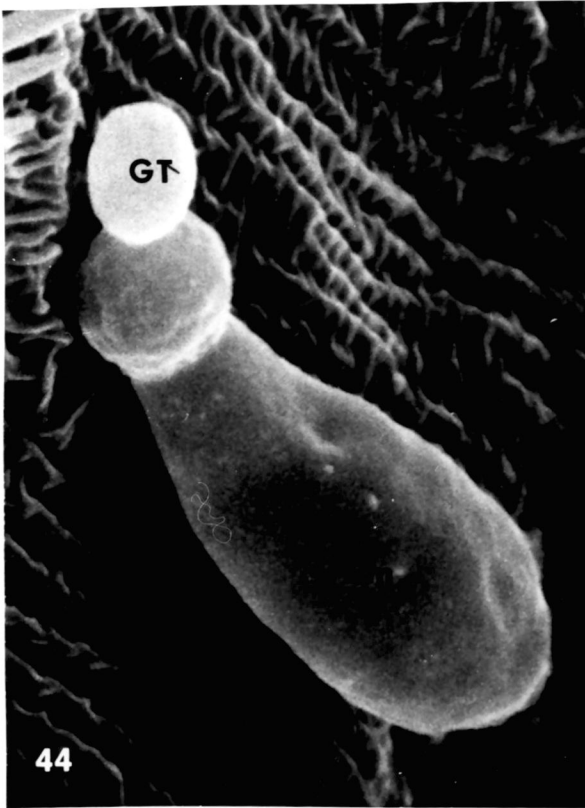
Figures 49-53. Germinating conidia. Approximate time (hours):
0, 1, 2, 8, and 11. 9,880x, 9,880x, 9,120x,
4,300x, and 4,000x, respectively. Cm,
conidium; GT, germ tube; GTi, germ tube
initial; sbp, subbasal peg.

49   sbp   1.0 μ

50   sbp   GTi   1.0 μ

51   GT   1.0 μ

52   Cm   GT   2.0 μ

53   2.0 μ
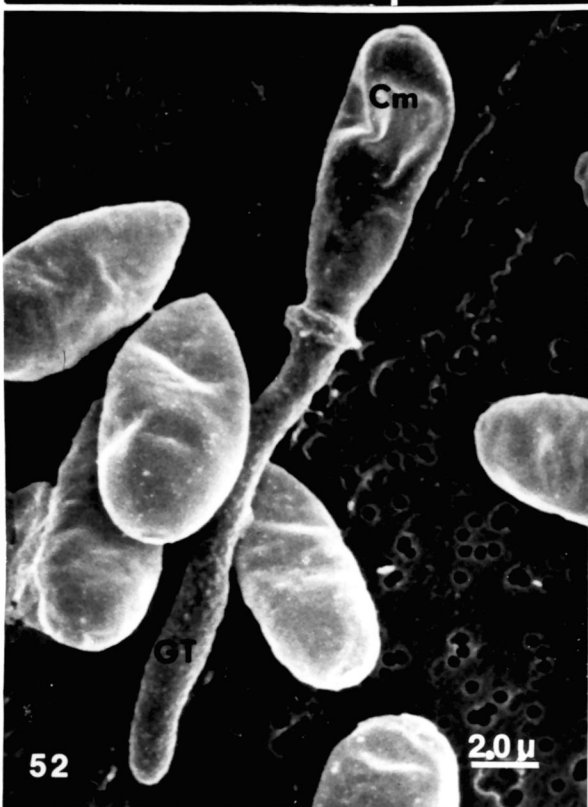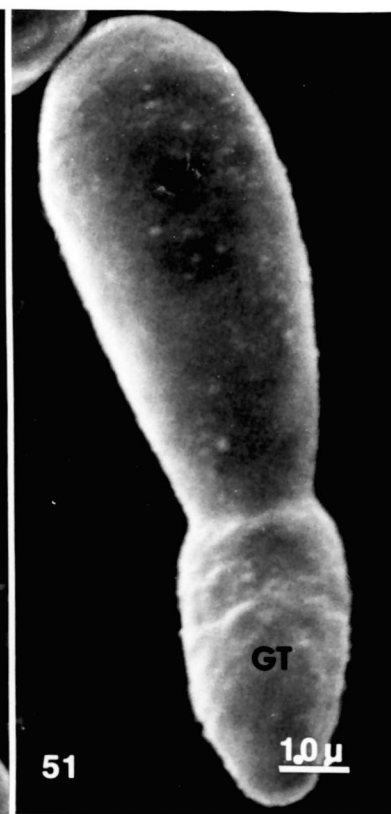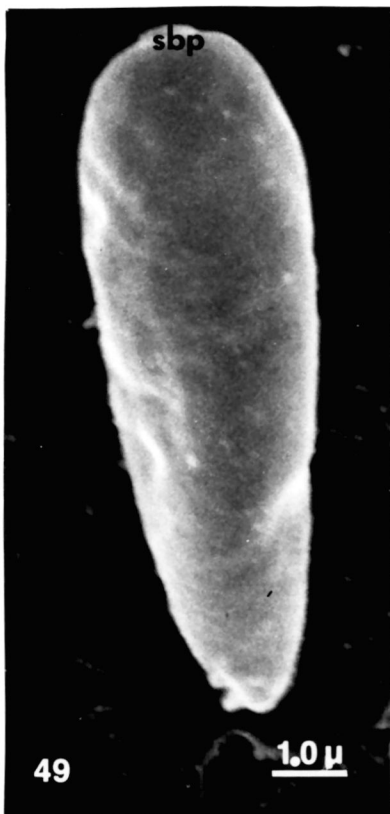
Figures 54(a-d).   Nomarski interference contrast
                    photomicrographs showing proliferation
                    of vegetative hyphae and rupture of the
                    anal gill epicuticle prior to
                    conidiogenesis. Approximate time:
                    (hours) 18, 24, 40, and 64 after conidial
                    adherence. 840x. Cm, conidium; Ep,
                    epicuticle; vh, vegetative hypha.

Figure 55.   Light micrograph showing hyphae that have
                    grown to pack the larval hemocoel. 35x.
                    Ab, abdomen; Ag, anal gills; He, head;
                    Si, siphon; Th, thorax.

Ep

vh

vh

Cm

100μ

54a   b   c   d

Si   Th   He

Ab

Ag
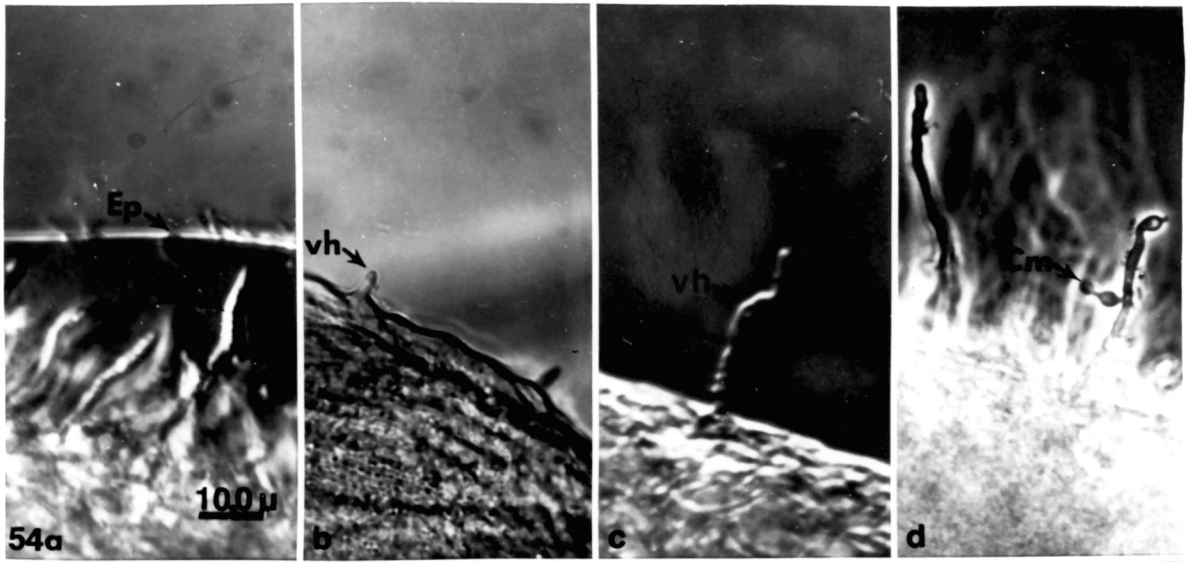
55   250.0μ

Figures 56-57. Scanning electron micrographs showing
          formation of conidia on vegetative hyphae that
          have ruptured the larval epicuticle. Note that
          no hyphae rupture the smooth thick epicuticle
          of the head. 210x and 290x, respectively.
          Ab, abdomen; He, head; Is, intersegmental
          region; Th, thorax.

Figure 58. Hyphal rupture of the epicuticle of the anal
          gills and lip around the anal pore. Note that
          no hyphae rupture the thick epicuticle of the
          siphon. 100x. Ag, anal gill; Ap, anal pore;
          Si, siphon.

Figure 59. Hyphal growth through anal pore and subsequent
          formation of conidia. 710x. Cm, conidium;
          vh, vegetative hypha.

56

He

Th

40.0 μ

57

Is

Ab

40.0 μ

58

Si

Ag

100 μ

59

200 μ
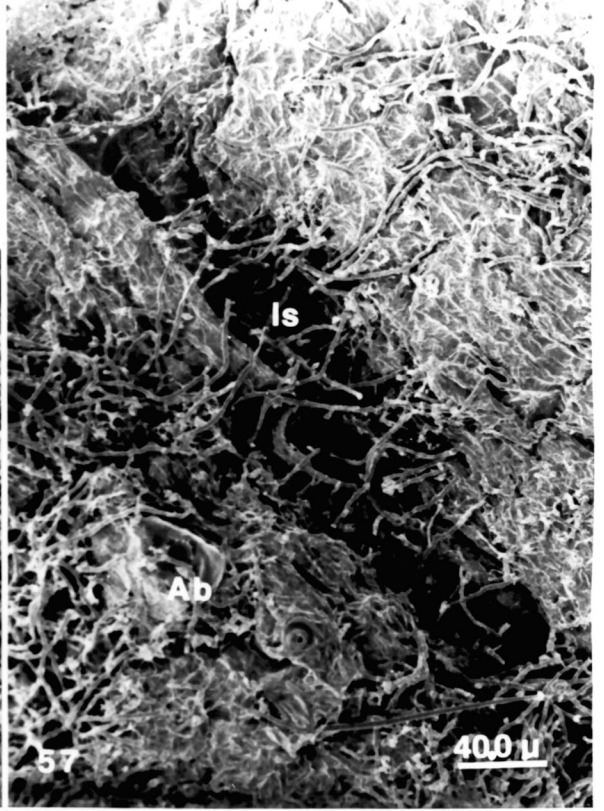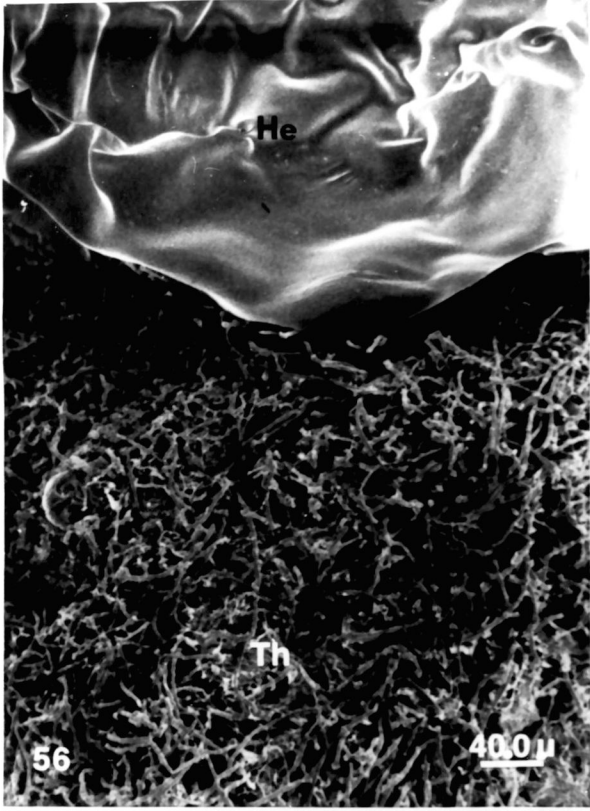
Figure 60.   Vegetative hyphae underlying the epicuticle.
             4,200x. Ep, epicuticle; H, hypha; V, vacuole.

Figure 61.   Rupture of the epicuticle by vegetative hypha.
             12,000x. Ep, epicuticle; H, hypha; M,
             mitochondrion; rep, ruptured epicuticle.

Figure 62.   Growth of vegetative hypha through the ruptured
             epicuticle. 9,240x. N, nucleus; rep, ruptured
             epicuticle; se, septum; V, vacuole.

Ep

V

H

60

2.0 μ

rep

Ep

H

M

61

1.0 μ

rep

V

rep

62
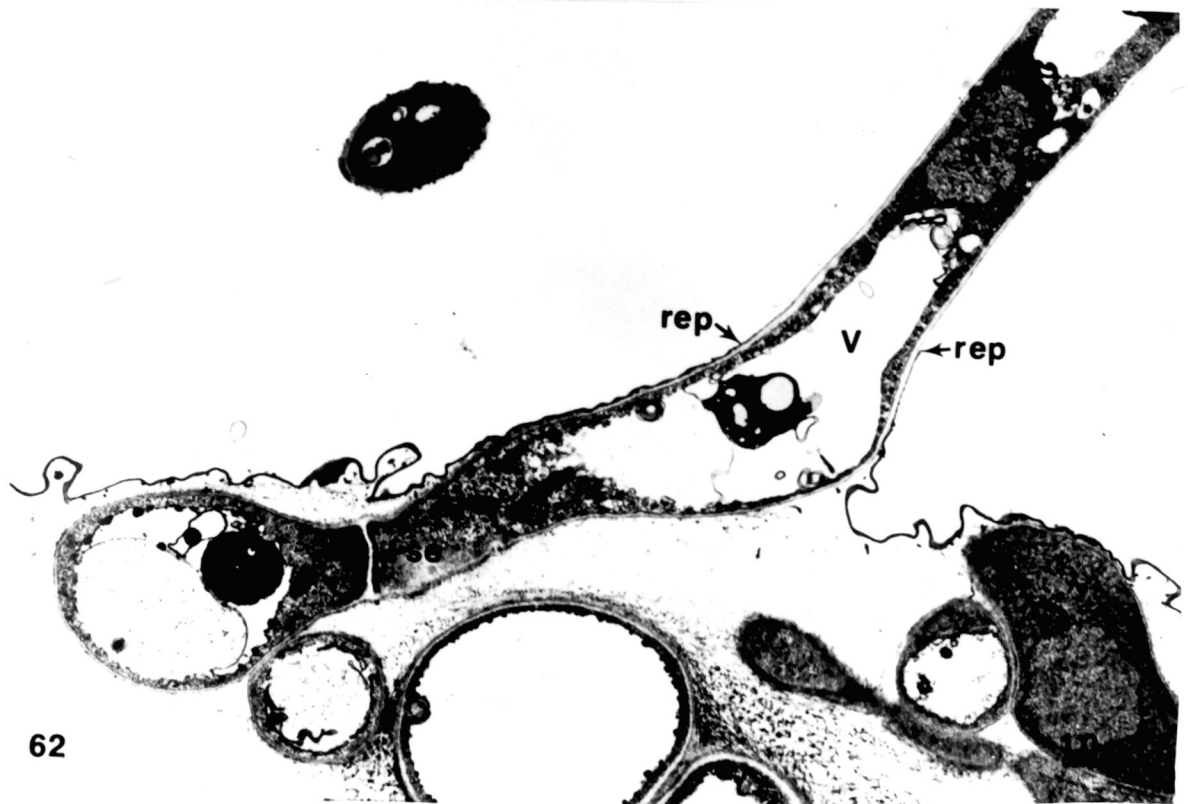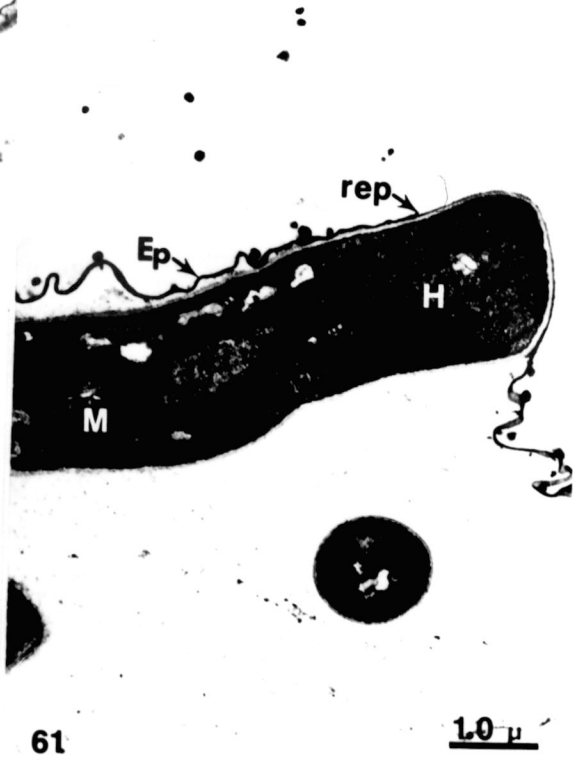
Figure 63(a-p). Nomarski interference contrast time-lapse

photomicrographs showing the sequence of

conidial formation. Arrows denote a common

point of reference. Time (hours): 0, 0.5,

2, 3, 3.5, 4, 4.5, 5.5, 6, 6.5, 7.5, 10.5,
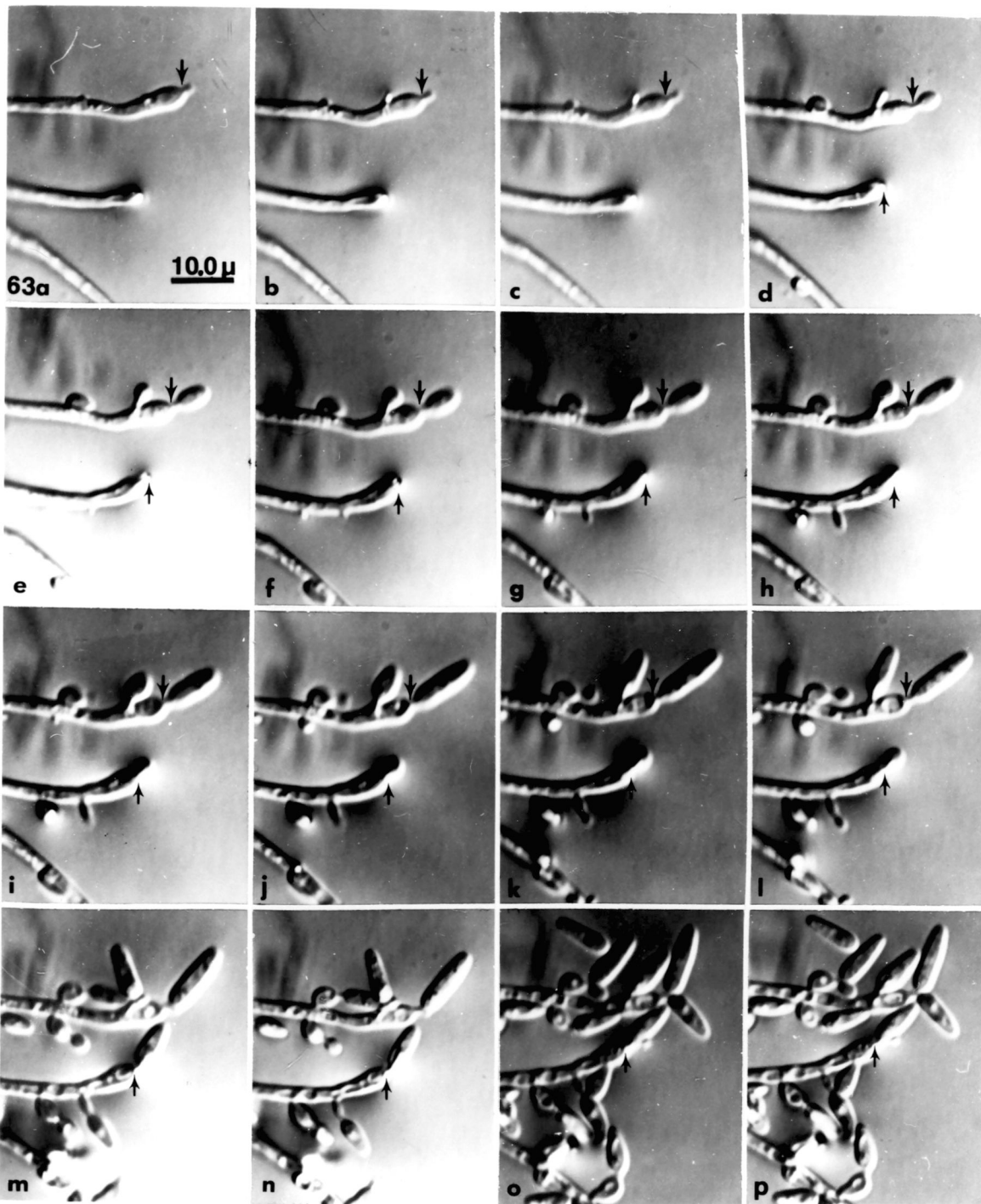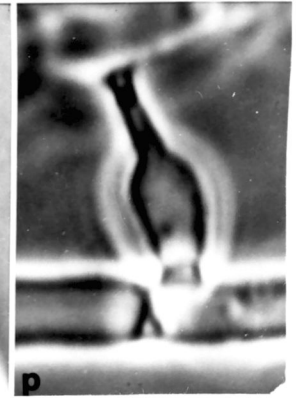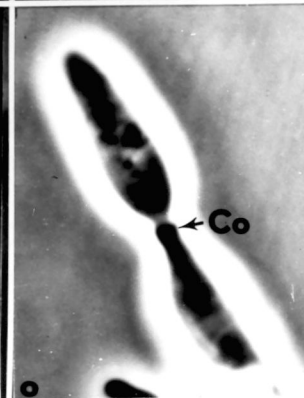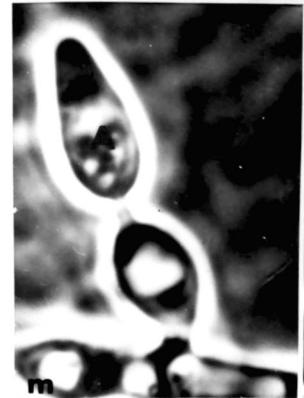
11.5, 12, 21, and 21.5. 1,040x.

63a 10.0 μ

Figure 64(a-p). Phase contrast photomicrographs showing
                 the sequence of conidial formation. 2,550x.
                 A, autophagosome; Cc, conidiogenous cell;
                 Ci, conidial initial; Cl, conidiogenous
                 locus; Co, collarette; gr, granular
                 region; H, hypha; St, sterigma.

64a. 4.0 μ
c. St→
d. Cc, H
e. Ci→
f. Cc, H
g. Cl→
o. Co→
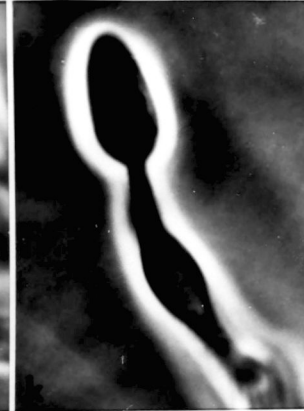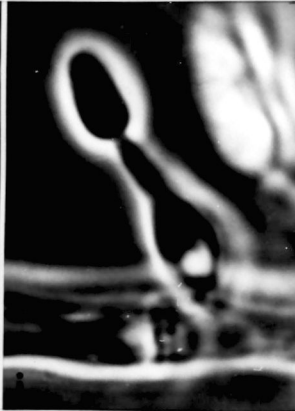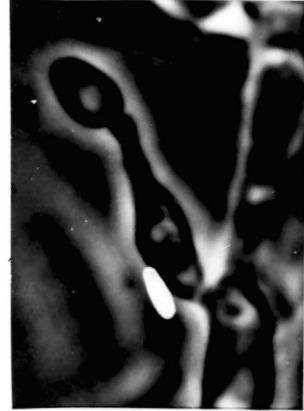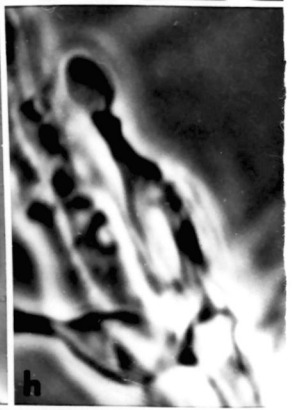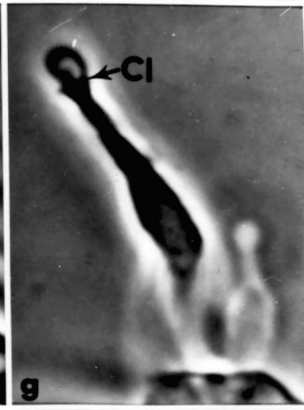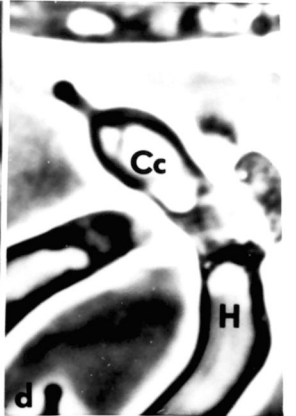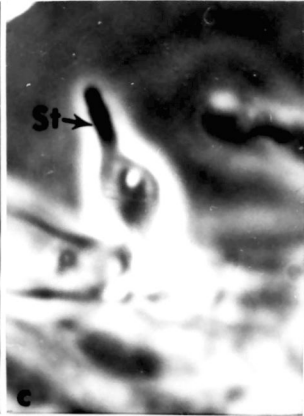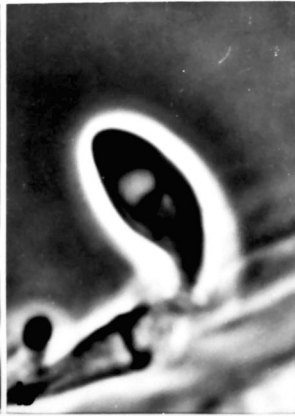
Figure 65. Transmission electron micrograph showing
conidiogenous cell arising laterally from the
vegetative hypha. 10,200x. Cc, conidiogenous
cell; H, hypha; se, septum.

Figure 66. Sterigma arising from distal apex of
conidiogenous cell. Note bilaminar wall of
conidiogenous cell. 11,900x. Cc, conidiogenous
cell; dl, dense wall layer; H, hypha; St, sterigma;
tl, translucent wall layer.

Figure 67. Scanning electron micrograph showing the
conidiogenous cell arising laterally from the
vegetative hypha. 9,800x. Cc, conidiogenous
cell; H, hypha.

Figure 68. Sterigma arising from the distal apex of the
conidiogenous cell. 9,800x. se, septum; St,
sterigma.

65

66

67

68
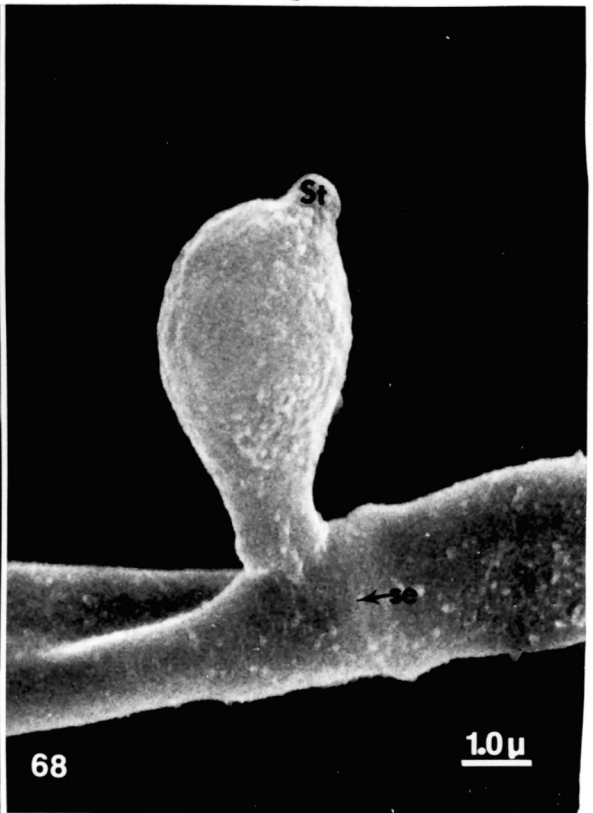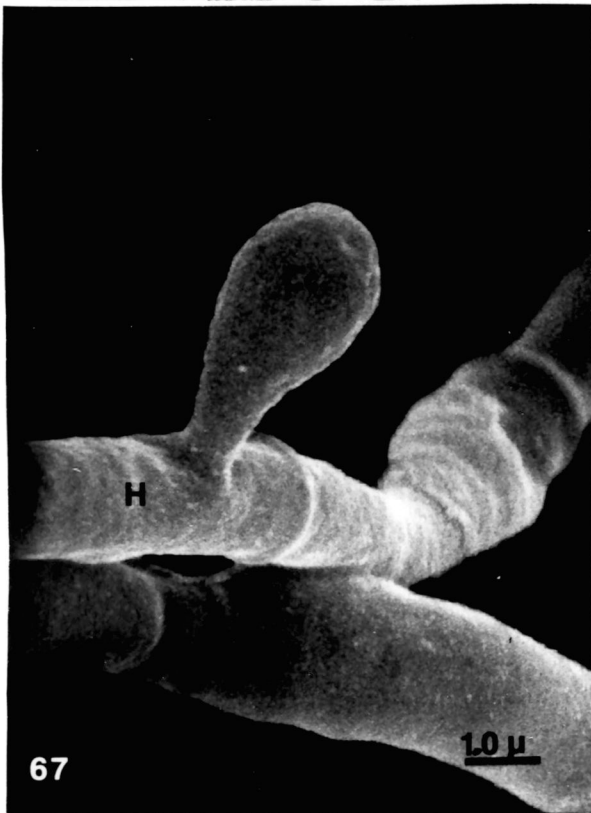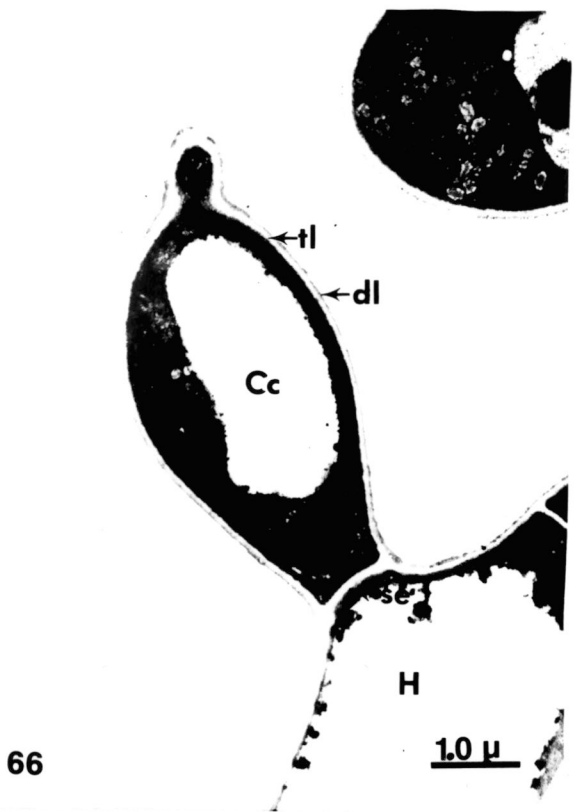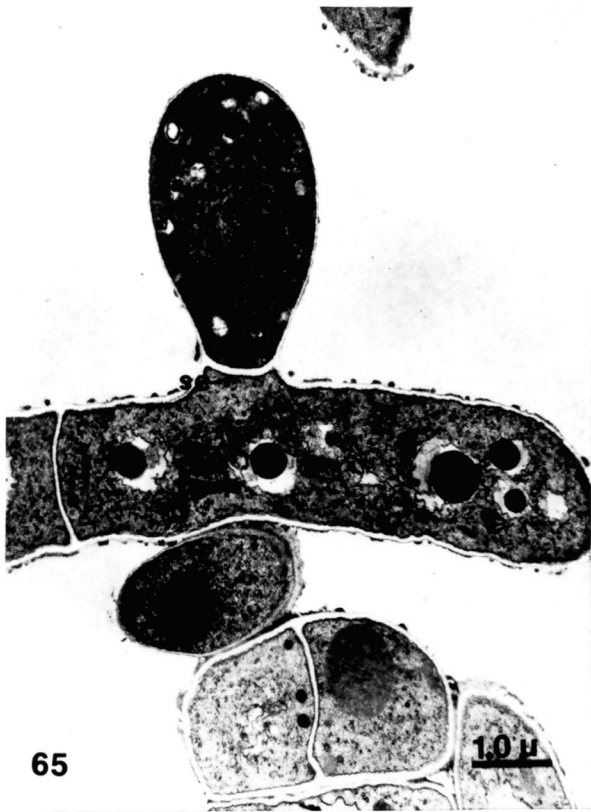
Figures 69-70. Transmission electron micrographs of
longitudinal sections through the conidial
initial and conidiogenous cell. Note
collarette at the conidiogenous locus.
17,000x. Cc, conidiogenous cell; Ci,
conidial initial; Cl, conidiogenous locus;
Co, collarette; dl, dense wall layer; L,
lipid body; M, mitochondrion; pwl, primary
wall layer; swl, secondary wall layer; tl,
translucent wall layer; wps, whorled
plasmalemmasome.

Figures 71-72. Scanning electron micrographs showing the
conidial initial arising from conidiogenous
cell. 12,600x. Cc, conidiogenous cell;
Ci, conidial initial; Cl, conidiogenous
locus; H, hypha; se, septum; St, sterigma.

swl

Co

Cl

L

0.5 μ   9

swl

pwl

tl

dl

0.5μ   70

Cl

71   1.0 μ

Ci

St

1.0 μ   72
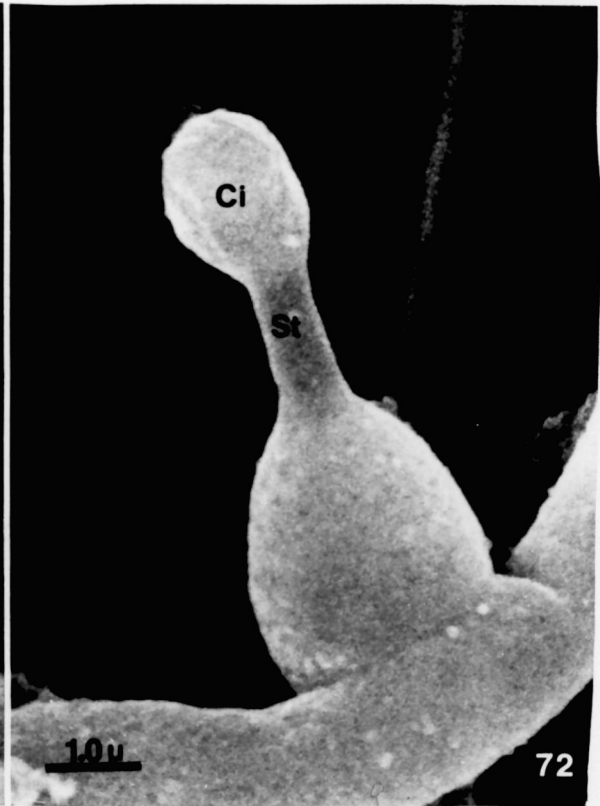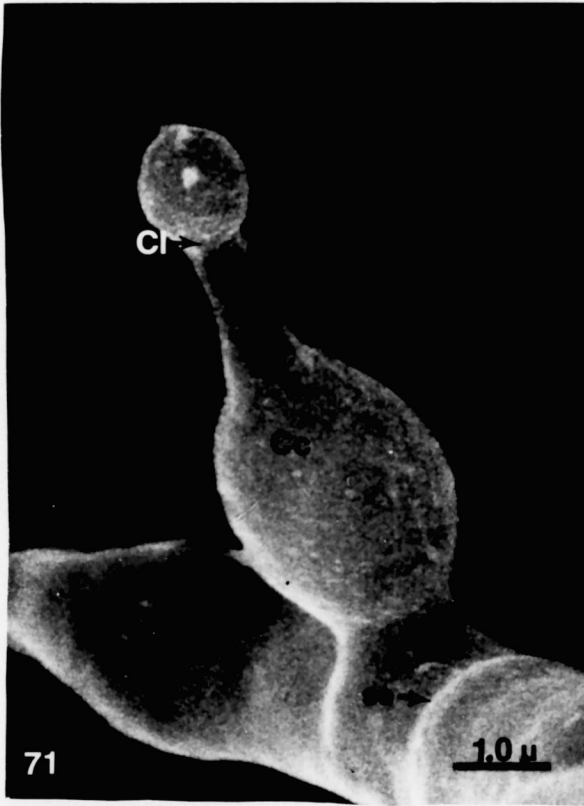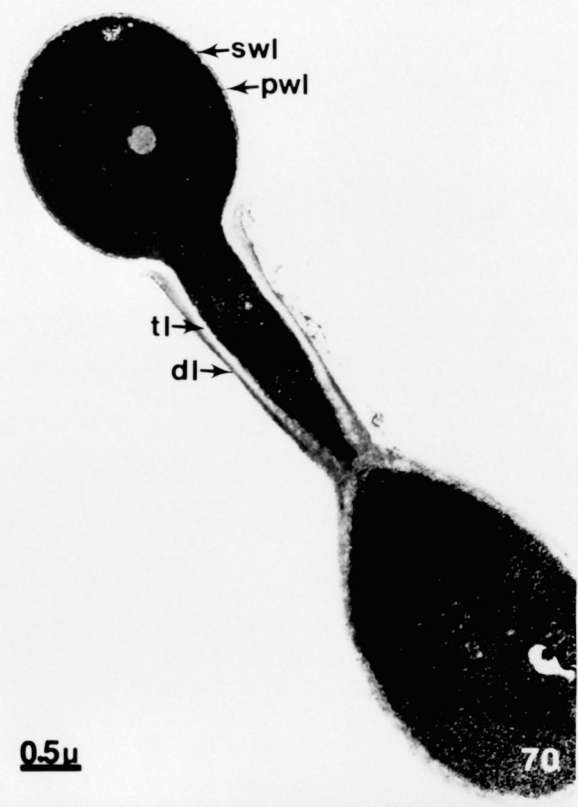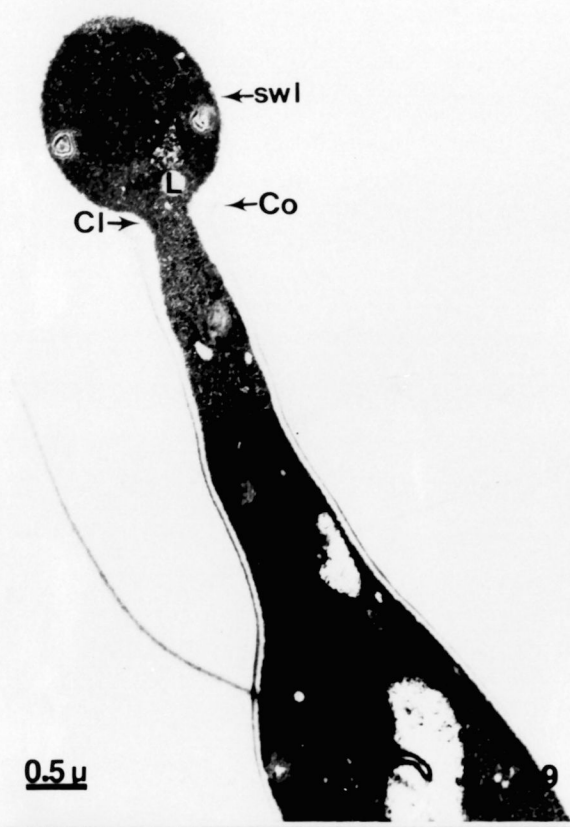
Figure 73. Immature conidium within which organelles are
developing. 17,000x. dbv, dense body vacuole;
ER, endoplasmic reticulum; L, lipid body; mvc,
multivesicular complex; pwl, primary wall layer;
swl, secondary wall layer; wps, whorled
plasmalemmasome.

Figure 74. Mature conidium delimited from the conidiogenous
cell by a septum. Note autophagosome located in
the proximal half of the conidium. 17,000x.
A, autophagosome; Cl, conidiogenous locus; dcv,
dense core vesicle; dl, dense wall layer; L,
lipid body; M, mitochondrion; sbp, subbasal peg,
se, septum; tl, translucent wall layer.

Figure 75. Conidium formed on terminal conidiogenous cell.
12,600x. Cc, conidiogenous cell; Cm, conidium;
St, sterigma.

Figure 76. Mature conidium borne on the conidiogenous cell.
Note wall remnants of the conidiogenous cell
adhering to the conidium. 12,600x. Cm, conidium;
wr, wall remnants.

73

pwl

swl

1.0 μ

74

A

L

Cl→ sbp ←se

tl→

dl→

1.0 μ

75

Cm

St

Co

1.0 μ

76

Cm

wr

1.0 μ

75
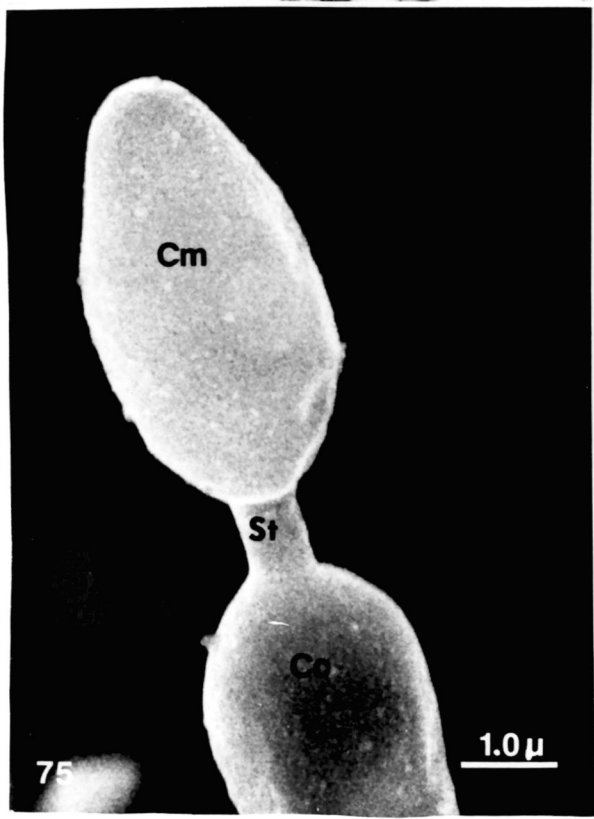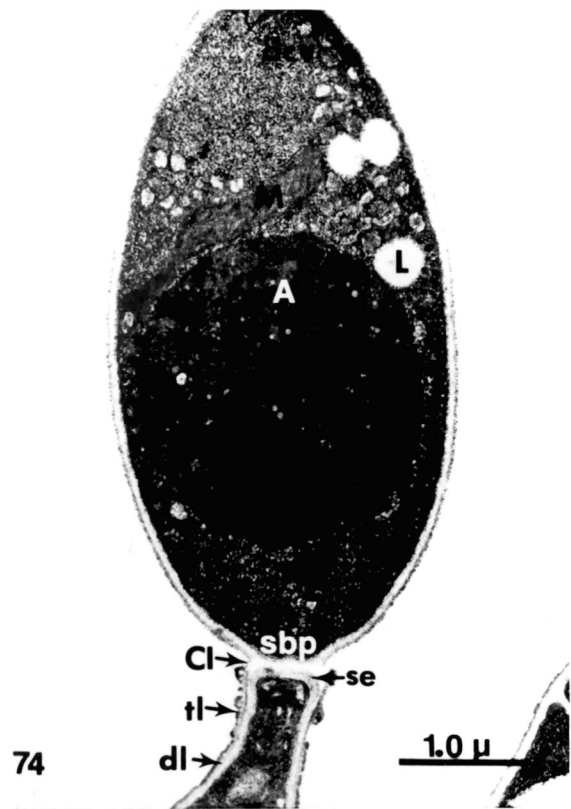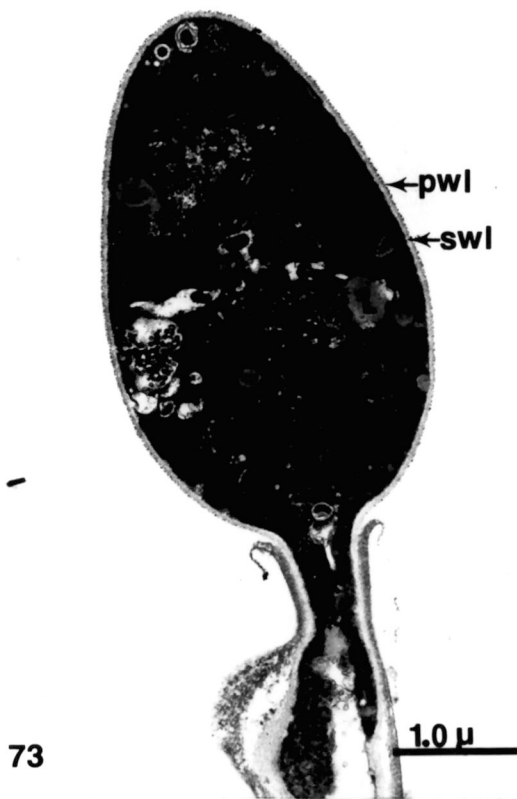
Figure 77. Mature conidium containing two autophagosomes.
Note wall remnants (collarette) at the base of
the conidium. 19,000x. A, autophagosome; dcv,
dense core vesicle; L, lipid body; sbp, subbasal
peg; se, septum; wps, whorled plasmalemmasome;
wr, wall remnants.

Figure 78. Branched conidiogenous cell giving rise to two
conidia. Note that autophagosome is absorbing
a lipid body. 11,900x. A, autophagosome; Ci,
conidial initial; dcv, dense core vesicle; gr,
granular region; L, lipid body; N, nucleus; sbp;
subbasal peg; wps, whorled plasmalemmasome.

Figure 79. Scanning electron micrograph of mature conidium.
Note prominent collarette around the conidial
base. 10,780x. wr, wall remnants.

Figure 80. Branched conidiogenous cell. Note that the
conidia are in different stages of development.
9,800x. Cc, conidiogenous cell; Ci, conidial
initial; Cm, conidium; wr, wall remnants.

77

78

79

80

77
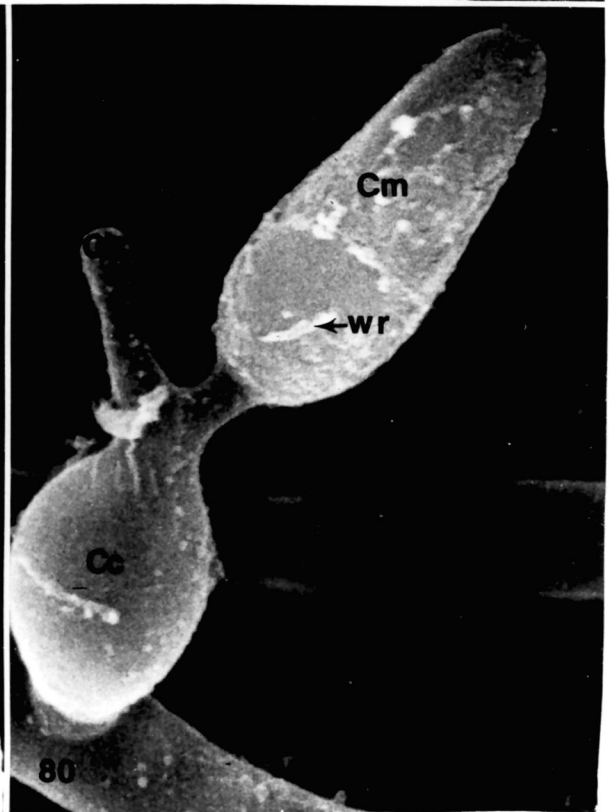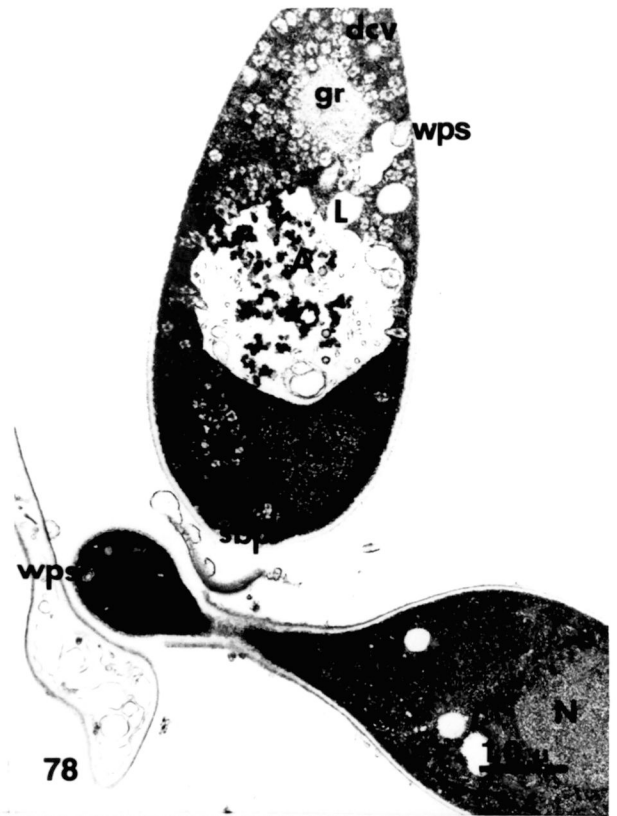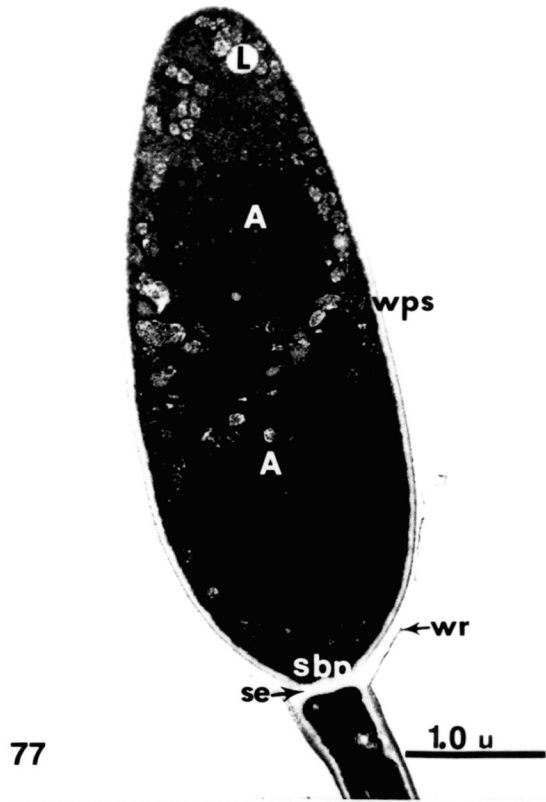
Figure 81 .   Dormant conidia containing typical cellular
              inclusions. Note mitochondria and ribosome
              packets within the autophagosomes. 17,500x.
              A, autophagosome; dcv, dense core vesicle; L,
              lipid body; M, mitochondrion; N, nucleus; rp,
              ribosome packet; wps, whorled plasmalemmasome.

Figure 82.   Mature conidium containing autophagosome.
              A, autophagosome; dcv, dense core vesicle; gb,
              granular body; L, lipid body; M, mitochondrion;
              N, nucleus; pwl, primary wall layer; swl,
              secondary wall layer; wps, whorled plasmalemmasome.

81

1.0 μ

82

1.0 μ
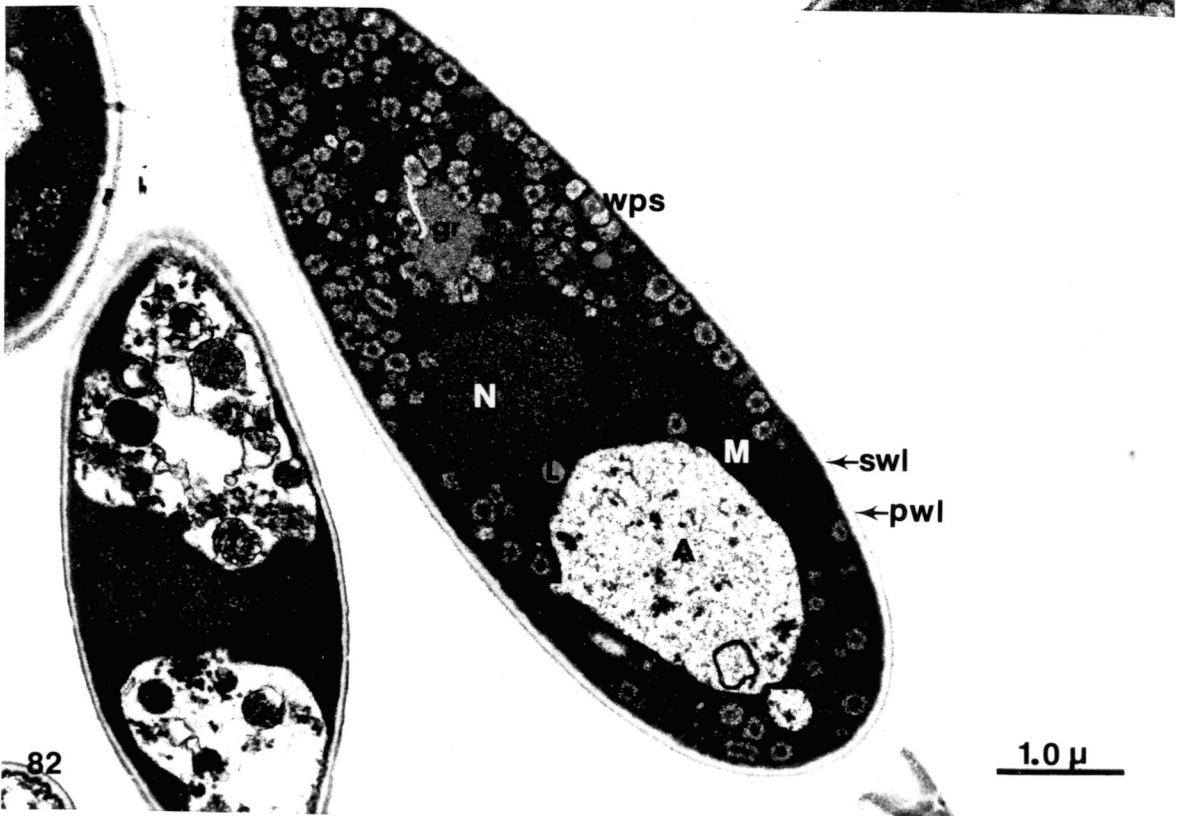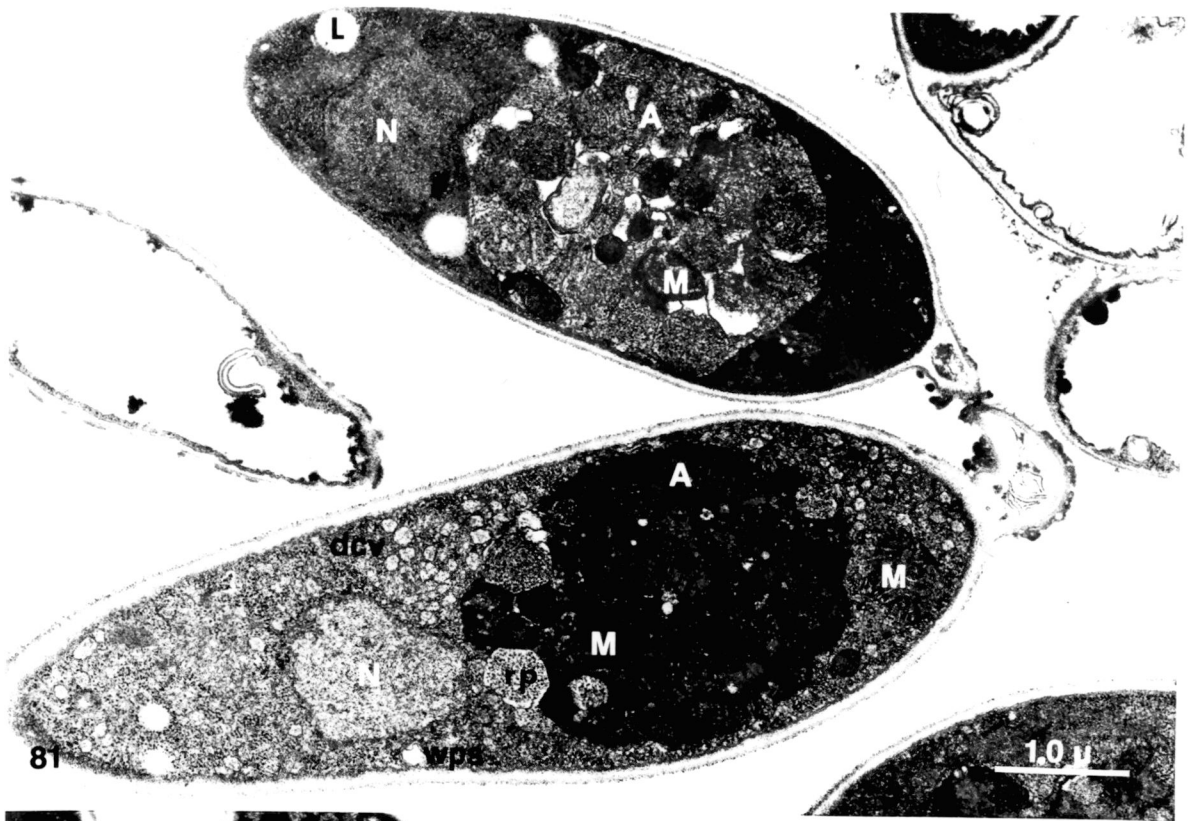
Figure 83. The two major types of conidiogenous cells.
Note the conidiogenous locus of the phialide
remains fixed while that of the annellide moves
distally.

PHIALIDIC

ANNELLIDIC

83

81
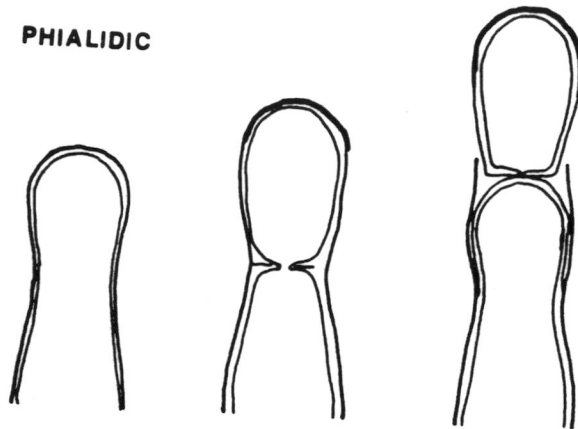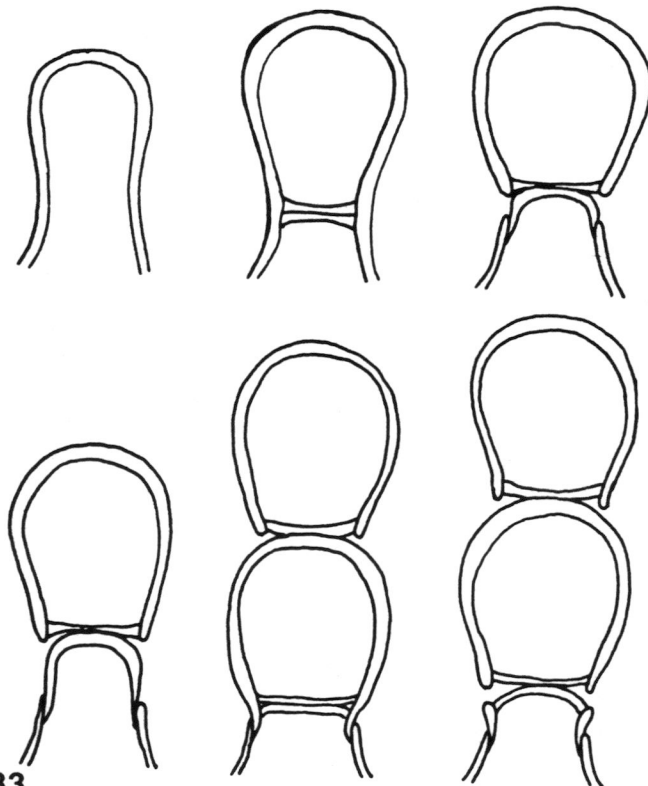
Figure 84. Developmental mode of conidia from the conidiogenous
cell. Note that thallic conidia enlarge only
after their delimitation by a septum.

BLASTIC
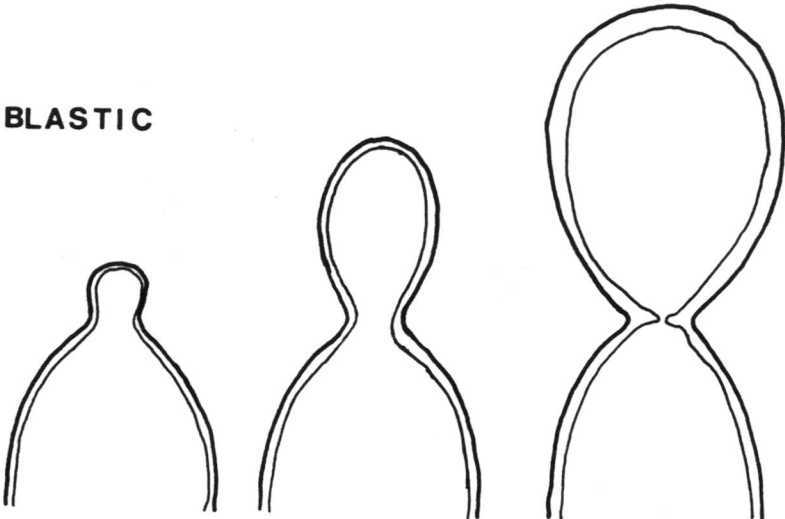
THALLIC
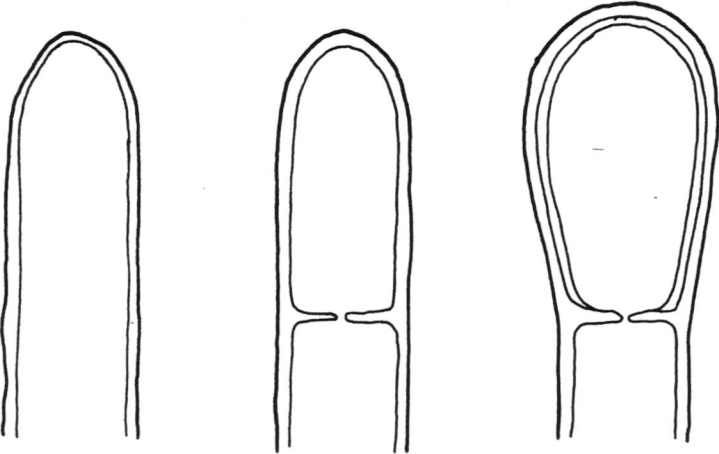
DISCUSSION

Laboratory Infection:

Techniques for laboratory infection of insect larvae by
fungal conidia vary according to the natural habitat of the
host and the corresponding site(s) of infection. For instance,
aquatic larvae are usually infected through the gut cuticle
following ingestion of water-borne conidia, while terrestrial
larvae are attacked through the epicuticle following contact
with air-borne conidia. In this regard, McCauley et. al.
(1968) applied a large number of Metarrhizium anisopliae
conidia to larval species of Elateridae with a camel's hair
brush. These terrestrial larvae were subsequently incubated
in individual 20 ml vials in which the relative humidity
exceeded 90%. During this incubation period, the fungus
infected the host by penetrating the sclerotized or membraneous
cuticle.

For Beauveria bassiana, application of conidia to
terrestrial insects (Lygus hesperus) (Dunn and Mechalas, 1963)
and aquatic mosquito larvae (Aedes aegypti, A. nigromaculis,
A. sierrensis, Anopheles albimanus, Culex pipiens, and C.
tarsalis) (Clark et. al., 1968) resulted in high mortalities
in the laboratory. In this case, twenty-five young adults of
L. hesperus confined to a pint carton screened at both ends
were subjected to 0.5 gm of a 5% conidial dust. Infection
was insured when the hosts were incubated under conditions
of 40-70% relative humidity. A more quantitative infection

technique was carried out by Clark et. al. (1968) on various species of mosquito larvae. For this, the larvae were placed in enamel pans (17 x 28 x 5 cm) containing one liter of water. Conidia were applied as a suspension or as a dust to the water surface at concentrations of approximately 1.77×10^6 conidia/liter (1.77×10^3 conidia/ml). Higher mortality rates were accomplished with the dust since the site of infection was the perisperacular lobes at the apex of the siphon. Larval death was presumably caused by asphyxiation.

Sweeney (1975a) used the basic techniques of Clark et. al. (1968) to infect larvae of _Culex fatigans_ with _Culicinomyces sp_. In this experiment, thirty to fifty larvae were placed in plastic trays containing approximately 200 ml of boiled river water. To the trays were added a conidial suspension containing an appropriate concentration of conidia (10^4- 10^6 conidia/ml) sufficient to kill the larvae. Sweeney (1973 and 1975b) also found this procedure caused the infection of _Anopheles_, _Aedes_, and _Culex_ larval species.

In the present study, the laboratory infection of _Aedes aegypti_ and _A. taeniorhynchus_ was carried out, with slight modifications, according to Sweeney (1975a). The number of larvae and the size of the container were reduced to facilitate observations of infected larvae. In addition, sterile distilled water was used rather than sterile river water for it was more convenient and offered comparable results.

Structure and Development:

The Conidium--Conidia of C. clavosporus bear some
morphological similarity to the single-celled conidia of
M. anisopliae and B. bassiana. The conidium of B. bassiana
is rounded to ovoid and borne singly on a small sterigma,
while that of M. anisopliae is long-ovoid to cylindrical
and produced in basipetal chains. Whole mounts of the
latter reveal a basal appendage not unlike although more
exaggerated than the subbasal peg of C. clavosporus. The
mature conidium of C. clavosporus is obclavate, single-celled,
and produced singly on a sterigma. It is bound by a bilaminate
wall comprised of a 0.1 µm thick electron-translucent,
granular inner (secondary wall) layer and a thin 0.03 µm
electron-dense striate outer (primary wall) layer.
Ultrastructural studies of conidia of Ascodesmis (Moore,
1963) and M. anisopliae (Zacharuk, 1970a) have revealed that
each was bound by two distinct wall layers not unlike those
of C. clavosporus. Zacharuk (1970a) reported that the
innermost wall layer of M. anisopliae, which is closely
applied to the plasma membrane, is electron-transparent,
faintly laminar to amorphous and of relatively uniform
thickness. Exteriorly, this layer blends into a more dense,
longitudinally striate wall layer that has a variable thickness
in individual conidia. Dormant conidia of M. anisopliae possess
a thin transparent layer covering the outer wall layer to which
is attached a sparse and irregular amorphous, mucoid substance

that presumably plays some role in the adhesion of conidia to the host cuticle (Zacharuk, 1970a). A coating that is probably similar in makeup and function also surrounds dormant conidia of C. clavosporus. Since this mucilaginous coating is rarely observed prior to conidial germination, it is probably formed immediately before germ tube initiation.

Moore (1963) suggested the outer conidial wall of Ascodesmis is secreted through the inner wall by the underlying plasma membrane and endoplasmic reticula. Zacharuk (1970a) feels this to also be true in M. anisopliae since the indentions and projections of the outer wall roughly coincide with those of the inner wall. Holding to this logic, it is likely that the outer primary wall of C. clavosporus is deposited through the inner secondary wall.

The dense core vesicles that apparently originate in the conidial apex are unique to the fully mature conidium of C. clavosporus. These inclusions migrate to become associated with the cell wall to perhaps secrete the thick electron-dense fibrillar coating that surrounds the dormant conidium. Ultrastructural observations of conidia in the early phases of germination show no signs of these vesicles, indicating they have perhaps been broken down within or excreted from the cell.

The most conspicuous inclusions within conidia of M. anisopliae are two large dense ovoid bodies that are each bound by a single membrane and positioned one on either side

of the centrally located nucleus. These bodies may contain
a nutrient store of heavy, possibly waxlike lipids. They
become less dense and finely granular during conidial
swelling early in the germination process. The central
contents of these bodies become coarsely granular, with
disappearance of the granules as germination progresses toward
germ tube formation. By the time the germ tube is initiated,
two large distinct vacuoles are present (Zacharuk, 1970a).
Hammill (1972) observed these "storage vacuoles" to initially
contain electron-dense particles that become homogenous in
appearance in older conidia. The proximal half of the mature
conidium of C. clavosporus contains a similar inclusion.
Prior to the complete maturation of the conidium,
multivesicular bodies arise, proliferate, and apparently fuse
to form one or two distinct double-membrane bound electron-
dense inclusions that are probably autophagosomes (autophagic
lysosomes). This is in apparent agreement with the feelings
of Kazama (1973), who postulated that multivesicular bodies
possibly differentiate into large cytolysosomes (autophagosomes).
In addition, he felt that they may be involved in the transport
of histolytic enzymes from the Golgi to these prominant
inclusions. Golgi bodies have also been linked to autolytic
activity in other fungi. In this regard, Mason and Wilson
(1978) reported them to be in the vicinity of and occasionally
attached to phagosomes in conidia of Elsinoe wisconsinensis.

The autophagosome in the mature conidium of C. clavosporus absorbs and subsequently breaks down cellular organelles, including lipid bodies, packets of ribosomes, endoplasmic reticula, and mitochondria. Electron micrographs taken by Zacharuk (1970a) show, in at least one instance, the "lipid inclusion" apparently absorbing an oil globule. In addition, the vacuolation he describes may actually be lipid bodies absorbed into this vacuole. The lipoidal and proteinaceous materials Hammill (1972) believes to be contained within these inclusions would be consistent with the partially digested residue of cellular components found in the autophagosome. The intravacuolar bodies observed in conidia of M. anisopliae are similar to the invaginations of the autophagic tonoplast in C. clavosporus.

Although autophagosomes have been most widely reported in animal cells, the inclusions have also been observed in the conidia of numerous species of mycetozoa. Ultrastructural studies of Stemonitis virginiensis (Mims, 1972), Didymium nigripes (Schuster, 1969), Dictyostelium discoideum and D. mucoroides (Maeda and Takeuchi, 1969) have revealed that the conidial autophagic lysosomes contain recognizable organelles such as mitochondria that appear in the process of digestion. Rhodin (1974) reports that the double membrane that encompasses these lysosomes to be characteristic of the autophagosome.

Adhesion of Conidia to Infection Sites--Infection via fungal conidia may occur through the epicuticle and/or the

gut cuticle of mosquito larvae. Fungal cysts of _Coelomomyces_ _psorophorae_ adhere in large numbers to the bases of the anal gills, in the intersegmental regions, around the anus, and on the head. The cysts are probably attracted to these areas by stimuli elicited from the host, possibly imposed by the cuticular textures (Travland, 1979). Soares (1979) reported that the imperfect fungus _Tolypodcladium_ _cylindrosporum_ usually infects mosquito larvae through the epicuticle, while the digestive tract acts as the secondary site of infection. Conidia of _C_. _clavosporus_ are presumably attracted to the host cuticle by a stimulus, perhaps thigmotrophic and/or nutrotrophic, elicited by the host. They adhere longitudinally to the gut cuticle, the primary infection site, in such a manner that their narrow apices are directed anteriorly. Such an orientation offers the least resistance to the moving food mass to help ensure conidial adherence (Sweeney, 1975a). Adherence of conidia to the infective sites is probably due to the electron-dense, fibrillar coating, presumably mucilaginous in nature, which encases mature conidia. Zacharuk (1970a) reported the sparse and irregular amorphous substance that surrounds conidia of _M_. _anisopliae_ to be mucoid in nature and so responsible for adhesion. This substance probably arises, however, from a sloughing of the inner, electron-transparent layer which may actually be responsible for conidial adherence.

Germination of Conidia--The conidium undergoes a
considerable amount of change with the initiation of the germ
tube growth. As germination proceeds, an electron-dense wall
layer (tertiary wall) that measures approximately 0.03 μm
thick separates slightly from the plasma membrane and becomes
evident. Zacharuk (1970a) described a similar such phenomenon
early in the germination of M. anisopliae conidia. Close
examination of the irregular plasmalemmasomes reveal that
these inclusions are formed by the invagination of the tertiary
wall as well as the plasma membrane. Hawker et. al. (1970)
suggest that these invaginations, present in Cunninghamella
elegans, may represent sites of enzyme activity which are
associated with a change in the chemical nature of the conidial
wall during germination. An alternative role is suggested by
the increased surface area of the plasmalemma in facilitating
the exchange of materials between the protoplasm and surrounding
environment (Steele and Fraser, 1973).

The secondary and tertiary wall layers in C. clavosporus
are continuous with the emerging germ tube while the primary
wall and mucilaginous coating are fractured. The germ tube,
which usually grows immediately toward the cuticle, is
probably attracted by a stimulus elicited from the host. In
M. anisopliae the germ tube is usually formed near one pole
of the conidium and grows laterally towards the cuticle,
particularly if the conidium is near this barrier.
This indicates a weak stimulus which operates over a distance

of only a few microns is emitted from the host (Zacharuk, 1970b). Unlike M. anisopliae, no appressorium is formed in C. clavosporus upon germ tube contact with the cuticle. A septum is sometimes formed at the base of the germ tube in both fungal species.

The digestion of cellular organelles within the autophagosome is largely carried out prior to germ tube formation and complete by the time this inclusion migrates to the proximal half of the conidium during germination. The inclusion, now considered a residual body, is at this stage bound by a poorly defined single membrane and contains the undigestible residue of cellular organelles. In M. anisopliae, Zacharuk (1970a) reported that the tonoplast of the "vacuole" breaks down once the germ tube is formed and its contents eventually become uniformly clear. Electron microscopy reveals that this residue migrates toward the tonoplast or, perhaps more often, coalesces into a fibrous electron-dense sphere within the residual body. This "microbody", clearly visible via light microscopy, exhibits rapid, presumably Brownian, movement. McCauley et. al. (1968) reported similar bodies in conidial vacuoles of M. anisopliae. In addition, Zacharuk (1971) observed similar electron-dense spheres within vacuoles of hyphae growing in moribund larvae. Zacharuk (1970a) postulated that these "microbodies" are the central remnants of the "lipid inclusion" or possibly a nucleus positioned alongside

the "vacuole". Once digestion is complete, the residue may be removed from the cell via exopinocytosis.

The mechanism of autophagy within conidia of C. clavosporus may play a role not only in the survival but also the development of the fungus. Ericsson (1969) suggests autophagic activity under normal functioning conditions is a mechanism by which cells remove worn-out organelles and recycles them into other cellular components. On the other hand, Hohl et. al. (1968) believe the autophagic vacuole of Acytostelium leptosomum to represent an energy source that ensures the survival of the conidium. Schuster (1969) speculates that the degraded protoplasmic material in the central vacuole of Didymium nigripes may serve as a food reserve. In studies with animal cells, Gaham (1967) and deDuve and Wattiaux (1966) have expressed the opinion that autophagy may turn out to be significant in the control of cellular activities, particularly during differentiation.

Cuticle Penetration--In C. clavosporus, a darkening of host tissue (melanization) was observed adjacent to the penetration sites and/or around the growing hyphae in larvae of Aedes aegypti and A. taeniorhynchus. A similar situation has been described for the infection of Astacus astacus by Aphanomyces astaci (Söderhäll et. al., 1979) and Culiseta inornata larvae by Coelomomyces psorophorae (Travland, 1979). Hyphae growing through the cuticle and throughout the hemolymph may become surrounded by a capsule secreted by

the host. Söderhäll et. al. (1979) reported that hyphae
within the hemolymph of arthropods are encapsulated by blood
cells. On the other hand, a capsule lacking blood cells
(humoral encapsulation) was secreted in the cuticle, hypodermal
cells, and hemolymph of Chironomus larvae in response to
invading hyphae of B. bassiana (Götz and Vey, 1974). Sweeney
(in press) reports that hyphae of Culicinomyces sp. growing
in larvae of Culex fatigans and Anopheles hilli were surrounded
by capsules of humoral origin. Both melanin and capsule
formation appear to be triggered by the fungal activation of
phenoloxidases within the host (Söderhäll et. al., 1979; and
Götz and Vey, 1974). Aoki and Yanase (1970) suggest that these
host defense responses occur only during moderate fungal
infections in which the phenoloxidase activity in the integument
may not be severely upset.

Cuticular penetration via the germ tube (penetrant hypha)
during larval infection by C. clavosporus is probably due
almost entirely to the action of histolytic enzymes released
from vesicles in the growing tip since no appressorial structure
is formed. The appressorium, formed at the growing tip of the
germ tube in such species as C. psorophorae, B. bassiana, and
M. anisopliae, functions not only to anchor the conidium but
also as a foundation to facilitate cuticular penetration
(Travland, 1979; Zacharuk, 1970). In M. anisopliae
the penetration peg arises from the appressorial pressure point
and pierces the cuticle via histolytic and mechanical action.

Although no distinct wall initially surrounds the peg, the
inner electron-transparent layer continuous with the
appressorial wall is later formed (Zacharuk, 1970c).

Once penetration has been accomplished by C. clavosporus
a collar of host tissue is formed around the penetrant hypha.
Travland (1979) observed such a collar in the infection of
C. inornata by C. psorophorae. The penetrant hypha grows to
a length of 3-6 µm into host tissue, is delimited by a septum,
and forms a spherical to ovoid hyphal cell from which one
vegetative hypha typically arises. This is similar to the
situation described by Zacharuk (1970c) in M. anisopliae
infections of Elateridae larvae. Once the penetration peg
pierces the epicuticle, it expands to form a discoid structure
called the penetration plate. Lateral penetration hyphae
arise from the plate once a septum has been formed across the
penetration peg. As in C. clavosporus, small, dense granules
are usually found in the vicinity of the septal pore on either
side of the septum. Zacharuk (1970c) feels that while the
granules found in M. anisopliae may be equated to the refractile
Woronin bodies of other fungi, they are possibly associated
with the formation of the large "lipoidal inclusions".

A clear zone devoid of tissue often observed around
penetrant hyphae of C. clavosporus may run the length of the
penetrant hypha, the hyphal cell, and the vegetative hypha(e).
In M. anisopliae, McCauley et. al. (1968) suggest the histolytic
enzymes that facilitate fungal penetration diffuse into the

integument directly from the appressorium. Zacharuk (1970c)
believes these enzymes to hydrolyze the epicuticle and outer
procuticle along the plasmalemma on the sides as well as tip
of the penetration peg and along the entire plasmalemma of
the penetration plate and the lateral penetration hyphae.

Hyphal Proliferation and Epicuticular Rupture--Once the
fungus has invaded the body cavity, vegetative hyphae branch
while consuming host tissue and bud laterally to give rise to
ovoid hyphal bodies. The hyphal bodies are presumably
distributed throughout the body by the hemolymph prior to
larval death in a manner similar to that described in the
infection of Galleria mellonella by B. bassiana and M. anisopliae
(Prasertphon and Tanada, 1968). Zacharuk (1970c and 1971)
reported a similar situation in the proliferation of M.
anisopliae in Elateridae larvae. He suggests the germination
of these scattered bodies results in the development of hyphae
in all parts of the body more rapidly than would be possible
by hyphal growth from the points of integument penetration.
Such would probably hold true in the infection by C.clavosporus.
Electron microscopy revealed thick-walled structures similar
to the chlamydospores Zacharuk (1971) observed in dead larvae.
The structures are perhaps involved primarily in the maintenance
of fungal viability within the host for extended periods during
unfavorable environmental conditions before the production of
external conidia (Zacharuk, 1971).

In C. clavosporus vegetative hyphae grow to pack the larval hemocoel and exert outward pressure on the epicuticle following the death of the larva. Initially, the pliable cuticle between the segments is ruptured. This is followed by epicuticular rupture of the anal gills, the abdomen, and the thorax. In the infection of Astacus astacus by Aphanomyces astaci (Unestam and Weiss, 1970) a hypha reaching the epicuticle from the inside always swells prior to outward penetration. Nyhlén and Unestam (1975) believed this swelling to take place during the time enzymes were breaking down the cuticle. Hyphal swelling has not been observed in C. clavosporus prior to epicuticular rupture.

Factors suggested as playing a role in the death of insects parasitized by fungi include: (1) histolytic action of the fungus; (2) toxin production; (3) mechanical blockage of the gut by mycelia; (4) damaging effect of the physical presence of the mycelia and (5) pathological changes in the hemolymph (McCauley et. al., 1968). It is probable that all five are causal factors in the death of mosquito larvae by C. clavosporus.

Conidiogenesis--Conidiogenesis in C. clavosporus is first evident when the lateral or terminal conidiogenous cells are initiated as evaginations of the emergent vegetative hyphae. Each evagination swells into a spherical to ovoid cell with the distal portion giving rise to typically one, but sometimes two sterigmata to form the characteristic flask-shaped

conidiogenous cell. In the electron-opaque region of the
sterigma immediately proximal to the conidiogenous locus,
the 0.1 μm thick electron-translucent granular wall of the
conidial initial is apparently synthesized and deposited.
A similar such region, apparent in the neck of the conidiogenous
cell of M. anisopliae (Hammill, 1972) and Trichoderma
saturnisporum (Hammill, 1974), presumably gives rise to the
cell wall of the conidial initial. The cytoplasm of the
conidiogenous cell swells to fracture the cell bilayer at the
apex of the sterigma and give rise to the conidial initial.
The wall of the conidiogenous cell is fractured in much the
same manner during the formation of the conidial initial of
M. anisopliae (Hammill and Wang, 1971). The fracture of this
bilayer results in a conspicuous structure, the collarette, at
the conidiogenous locus. The presence of this collarette,
although sometimes inconspicuous (as in M. anisopliae), is
indicative of the de nova cell wall synthesis and the "blowing
out" of the conidial initial. The conidiogenous cell of
C. clavosporus is therefore a phialide. This ultrastructural
evidence supports the earlier light microscope observations
of Sweeney (1975a).

As the conidial initial develops, a thin electron-dense
striate wall layer is deposited outside the electron-translucent
layer. Hammill (1972) reported that the electron-transparent
inner layer and electron-dense outer layer of the conidial
initial of M. anisopliae were readily visible when the

"blowing out" of the conidial initial was begun. Once the conidium of C. clavosporus reaches maturity, a septum is formed between the phialide mouth and the subbasal peg of the conidium at the conidiogenous locus. An abscission zone is formed between the septum and the subbasal peg that allows the conidium to be easily dislodged from the phialide. In Stachybotrys atra, Campbell (1972) reported that the conidium broke away from the phialide as the septum split into two layers; one layer forming the base of the conidium and the other covering the opening at the phialide tip.

Classification--Classification of fungi within the Deuteromycetes (Fungi Imperfecti) has historically been a very difficult if not impossible task. The perfect (sexual) stage conventionally used in fungal classification is either unknown or completely lacking in the Deuteromycetes. To further complicate matters, fungi in this class produce several distinct types of conidia. The two major schemes for classifying the Fungi Imperfecti will be briefly discussed.

The Saccardoan System, which depends on the size, shape, color, septation, and attachment of conidia as criteria for classification, is convenient for it is not only simple but comprehensive in nature. However, this system has fallen into disfavor in recent years primarily due to the following: (1) the morphological characters used in classification are often modified by changing environmental conditions, such as those provided under culture conditions; and (2) it is an

artificial classification scheme. As a result, various workers such as Hughes (1953), Subramanian (1962), Tubaki (1963), and Barron (1968) have utilized conidial ontogeny as a basis for a modern classification system.

Classification employing the most widely accepted scheme, the Hughes-Tubaki-Barron System, depends on identifying the type of conidiogenous cell as well as the developmental mode of conidia (conidiogenesis) from that cell. A phialide is a conidiogenous cell that produces conidia in a basipetal fashion from an open end with no detectable increase in length; i.e., the conidiogenous locus is more or less fixed. The other major type of conidiogenous cell is the annellide. The conidiogenous locus is not fixed, therefore causing the cell to elongate with the formation of each conidium (Figure 83). The developmental mode of conidia may be described as either blastic or thallic. A blastic conidium arises from only a portion of a preexisting cell and undergoes significant enlargement before it is delimited from the conidiogenous cell. The thallic mode is defined as an entire preexisting hyphal cell that is transformed into a conidium. Thallic conidia enlarge only after their delimination by a septum (Figure 84). Additional categorization of developmental patterns is based on wall relations between the conidium and conidiogenous cell. If the outer wall of the cell ruptures and separates from the inner conidial wall, the development is enteroblastic or enterothallic. If, however, the outer wall remains continuous

to encompass the mature conidium, the process is holoblastic
or holothallic. Although subtle problems do remain, the
Hughes-Tubaki-Barron System is being effectively utilized
in the Hyphomycetes (Moniales).

The conidiogenous locus in C. clavosporus as revealed
by time-lapse photomicrographs does not move appreciably
proximally or distally during the formation of the conidium.
This indicates, along with the presence of the collarette at
the conidiogenous locus, that the conidiogenous cell of
C. clavosporus is a phialide. Cytoplasm migrates across the
open mouth of the phialide into the growing conidium. A
septum is formed between the phialide mouth and the subbasal
peg once the obclavate conidium has reached maturity. The
evidence therefore alludes that the mode of conidial development
is enteroblastic-phialidic. This, along with the fact that
the lateral conidiogenous cell is not present on a
differentiated supportive hypha, suggests that C. clavosporus
can be placed in Section IV B according to the Hughes-Tubaki-
Barron classification scheme.

Biological Control:

Culicinomyces clavosporus, effective against mosquitos
in laboratory and field trials, is currently the leading
candidate as a biological control agent of these pests. Unlike
Beauveria bassiana or Metarrhizium anisopliae, this fungus
yields predictable mortality rates and has not been found to

infect or elicit allergic responses from warm-blooded animals. In addition, it controls mosquito populations much more effectively than <u>Beauveria</u> or <u>Metarrhizium</u>. Once improvements are made in conidial formulations and application, <u>C</u>. <u>clavosporus</u> may replace chemical insecticides in some areas as the primary agent of mosquito control.

REFERENCES CITED

Alexopoulos, C. J., and C. W. Mims. 1979. Introductory Mycology. John Wiley & Sons, Inc., New York. 632 pp.

Aoki, J., and K. Yanase. 1970. Phenol oxidase activity in the integument of the silkworm Bombyx mori infected with Beauveria bassiana and Spicaria fumoso-rosea. J. Invert. Pathol. 16:459-464.

Barnett, H. L., and B. B. Hunter. 1972. Illustrated genera of imperfect fungi. 3rd edition. Burgess Publishing Company, Minneapolis. 241 pp.

Bechtel, D. B. 1976. Nuclear degeneration in the Myxomycete Physarella oblonga. Protoplasma. 90:179-187.

Bronchart, R., and V. Demoulin. 1975. Septum ultrastructure of Ostracoderma torrendii. Can. J. Bot. 53(15):1549-1553.

Campbell, R. 1972. Ultrastructure of conidium ontogeny in the Deuteromycete fungus Stachybotrys atra Corda. New Phytol. 71:1143-1149.

Capanna, E. 1973. Lysosomes. P. Gray, ed. In: The Encyclopedia of Microscopy and Microtechnique. Van Nostrand Reinhold Company, New York.

Charvat, I., I. K. Ross, and J. Cronshaw. 1973. Ultrastructure of the plasmodial slime mold Perichaena vermicularis. Protoplasma. 76:333-351.

Cole, G. T. 1975. The thallic mode of conidiogenesis in the Fungi Imperfecti. Can. J. Bot. 53:2983-3001.

Cole, G. T., and W. B. Kendrick. 1968. A thin chamber for time-lapse photomicrography of fungi at high magnifications. Mycologia. 60:340-344.

Cole, G. T., and W. B. Kendrick. 1969. Conidium ontogeny in hyphomycetes. The phialides of Phialophora, Penicillium, and Ceratocystis. Can. J. Bot. 47(5):779-789.

Cole, G. T., and R. A. Samson. 1979. Patterns of Development in Conidial Fungi. Pitman Publishing Limited, London. 190 pp.

Couch, J. N., S. W. Romney, and B. Rao. 1974. A new fungus which attacks mosquitos and related Diptera. Mycologia. 66:374-379.

Debenham, M. L., and R. C. Russell. 1977. The insect pathogenic fungus Culicinomyces in adults of the mosquito Anopheles amictus hilli. J. Aust. Ent. Soc. 16:46.

de Duve, C., and R. Wattiaux. 1966. Function of lysosomes. Ann. Rev. Physiol. 28:435-492.

Egerton, J. R., W. J. Hartley, R. C. Mulley, and A. W. Sweeney. 1978. Susceptibility of laboratory and farm animals and two species of duck to the mosquito fungus Culicinomyces sp. Mosquito News. 38(2):260-263.

Ericsson, J. L. E. 1969. Cellular autophagy. J. T. Dingle and H. B. Fell, eds. In: Lysosomes in Biology and Pathology. Vol. 2. North-Holland Publishing Co., London. pp. 345-394.

Gaham, P. B. 1967. Histochemistry of lysosomes. Intern. Rev. Cytol. 21:1-63.

Glover, S. U., and R. T. Hanlin. 1981. Ultrastructure of conidiogenesis in Sphaerostilbe ochracea. Amer. J. Bot. 68(5):685-696.

Götz, P., and A. Vey. 1974. Humoral encapsulation in Diptera (Insecta): Defense reactions of Chironomus larvae against fungi. Parasitology. 68:193-205.

Hammill, T. M. 1972. Electron microscopy of phialoconidiogenesis in Metarrhizium anisopliae. Am. J. Bot. 59:317-326.

Hammill, T. M. 1974. Electron microscopy of phialides and conidiogenesis in Trichoderma saturnisporum. Am. J. Bot. 61:15-24.

Hammill, T. M., and C. J. K. Wang. 1971. Fine structure of phialoconidiation in Metarrhizium anisopliae (Hyphomycetes). Am. J. Bot. 58:474.

Hawker, L. E., B. Thomas, and A. Beckett. 1970. An electron microscope study of structure and germination of conidia of Cunninghamella elegans Lender. J. Gen. Microbiol. 60:181-189.

Hohl, H. R., S. T. Hamamoto, and D. E. Hemmes. 1968. Ultrastructural aspects of cell elongation, cellulose synthesis, and spore differentiation in Acrostelium leptosomum, a cellular slime mold. Amer. J. Bot. 55:783-796.

Kazama, F. 1973. Ultrastructure of Thraustochytrium sp. Zoospores. III. Cytolysosomes and Acid Phosphatase Distribution. Arch. Mikrobiol. 89:95-104.

Kendrick, B. (ed.). 1971. Taxonomy of Fungi Imperfecti. University of Toronto Press, Toronto.

Kozakiewicz, Zofia. 1978. Phialide and conidium development in the Aspergilli. Trans. Br. Mycol. Soc. 70(2):175-186.

Maeda, Y., and I. Takeuchi. 1969. Cell differentiation and fine structures in the development of cellular slime molds. Development, Growth, and Differentiation. 11:232-245.

Mason, D. L., and C. L. Wilson. 1978. Fine-structure analysis of host-parasite relations in the Spot Anthracinoise of Desmodium. Cytology and Histology. 68:65-73.

Matile, P. 1975. The lytic compartment of plant cells. I. Springer-Verlay, New York. pp. 76-86.

McCauley, V. J. E., R. Y. Zacharuk, and R. D. Tinline. 1968. Histopathology of green muscardine in larvae of four species of Elateridae (Coleoptera). J. Invert. Pathol. 12:444-459.

Mims, C. W. 1972. Centrioles and golgi apparatus in postmeiotic spores of the Myxomycete Stemonitis virginiensis. Mycologia. 64:452-456.

Nyhlén, L., and T. Unestam. 1975. Ultrastructure of the penetration of the crayfish integument by the fungal parasite, Aphanomyces astaci, Oomycetes. J. Invert. Pathol. 26:353-366.

Powell, M. J. 1976. Ultrastructural changes in the cell surface of Coelomomyces punctatus infecting mosquito larvae. Can. J. Bot. 54:1419-1437.

Prasertphon, S., and Y. Tanada. 1968. The formation and circulation, in Galleria, of hyphal bodies of entomophthoraceous fungi. J. Invert. Pathol. 11:260-280.

Reynolds, E. S. 1963. The use of lead citrate at high pH as an electron-opaque stain in electron microscopy. J. Cell Biol. 17:208.

Rhodin, J. A. 1974. Histology, a text and atlas. Oxford University Press, New York.

Roberts, D. W. 1973. Means for insect regulation: Fungi. Annals of the New York Academy of Sciences. 217:76-84.

Russell, R. C., M. L. Debenham, and D. J. Lee. 1979. A natural habitat of the insect pathogenic fungus Culicinomyces in the Sidney area. Proc. Linn. Soc. N.S.W. 103:71-73.

Schuster, F. L. 1969. Nuclear degeneration during spore formation in the true slime mold, Didymium nigripes. J. Ultrastruct. Res. 29:171-181.

Soares, G. G. Jr. 1979. A study of Tolypocladium cylindrosporum Gams, a new naturally occurring fungal pathogen of mosquitos (with notes on Beauveria bassiana ((Bals.) Vuill.)). Ph.D. dissertation, University of California, Berkeley. 177 pp.

Söderhäll, K., L. Hall, T. Unestam, and L. Nyhlén. 1979. Attachment of phenoloxidase to fungal cell walls in arthropod immunity. J. Invert. Pathol. 34:285-294.

Steele, S. D., and T. W. Fraser. 1973. Ultrastructural changes during germination of Geotrichum candidum arthrospores. Can. J. Bot. 19(8):1031-1034.

Sweeney, A. W. 1975a. The mode of infection of the insect pathogenic fungus Culicinomyces in larvae of the mosquito Culex fatigans. Aust. J. Zool. 23:49-59.

Sweeney, A. W. 1975b. The insect pathogenic fungus Culicinomyces in mosquito and other hosts. Aust. J. Zool. 23:59-64.

Sweeney, A. W. 1977a. Infection of aseptically reared mosquito larvae with Culicinomyces sp. J. Invert. Pathol. 30:273.

Sweeney, A. W. 1977b. The pathogenicity of the fungus Culicinomyces to mosquito larvae in a natural field habitat. J. Med. Entomol. 14(4):495-496.

Sweeney, A. W. 1978a. The effects of temperature on the mosquito pathogenic fungus Culicinomyces. Aust. J. Zool. 26:47-53.

Sweeney, A. W. 1978b. The effects of salinity on the mosquito pathogenic fungus Culicinomyces. Aust. J. Zoo. 26:55-59.

Sweeney, A. W. 1979a. Further observations on the host range of the mosquito fungus Culicinomyces. Mosquito News. 39(1):140-142.

Sweeney, A. W. 1979b. Infection of mosquito larvae by
   Culicinomyces sp. through anal papillae. J. Invert.
   Pathol. 33:249-251.

Sweeney, A. W. 1980. Prospects for the use of Culicinomyces
   fungi for biocontrol of mosquitos. M. Laird, ed. In:
   Biocontrol of Medical and Veterinary Pests. Praegar
   Scientific Publishers, New York.

Sweeney, A. W. (in press). Fungal pathogens of mosquito
   larvae. E. W. Davidson, ed. In: Pathogenesis of
   Invertebrate Microbial Diseases. Allanheld Osmum Inc.,
   Montrose, New Jersey.

Sweeney, A. W., D. J. Lee, C. Panter, and L. W. Burgess.
   1973. A fungal pathogen for mosquito larvae with
   potential as a microbial insecticide. Search. 4(8):
   344-345.

Sweeney, A. W., R. G. Wright, and L. van der Lubbe. 1980.
   Ultrastructural observations on the invasion of mosquito
   larvae by the fungus Culicinomyces. Micron. 11:487-488.

Thorton, R. M. 1968. The fine structure of Phycomyces.
   I. Autophagic vesicles. J. Ultrastruct. Res. 21:269-280.

Travland, L. B. 1979. Initiation of infection of mosquito
   larvae (Culiseta inornata) by Coelomomyces psorophorae.
   J. Invert. Pathol. 33:95-105.

Unestam, T., and D. W. Weiss. 1970. The host-parasite
   relationship between freshwater crayfish and the crayfish
   disease fungus Aphanomyces astaci: Responses to infection
   by a susceptible and a resistant species. J. Gen.
   Microbiol. 60:77-90.

Vey, A., and J. Fargues. 1977. Histological and ultrastructural
   studies of Beauveria bassiana infection in Leptinotarsa
   decemlineta larvae during ecdysis. J. Invert. Pathol.
   30:207-215.

Woronin, M. 1866. Senkenbergischen Naturforsch. Ges. 5:333.

Yasuo, M., and I. Takeuchi. 1969. Cell differentiation and
   fine structures in the development of the cellular slime
   molds. Dev., Growth, and Diff. 11(3):232-245.

Zacharuk, R. Y. 1970a. Fine structure of the fungus
   Metarrhizium anisopliae infecting three species of larval
   Elateridae (Coleoptera): I. Dormant and germinating
   conidia. J. Invert. Pathol. 15:63-80.

Zacharuk, R. Y. 1970b. Fine structure of the fungus
    Metarrhizium anisopliae infecting three species of
    larval Elateridae (Coleoptera): II. Conidial germ
    tubes and appressoria. J. Invert. Pathol. 15:81-91

Zacharuk, R. Y. 1970c. Fine structure of the fungus
    Metarrhizium anisopliae infecting three species of
    larval Elateridae (Coleoptera): III. Penetration of
    the host integument. J. Invert. Pathol. 15:372-396.

Zacharuk, R. Y. 1971. Fine structure of the fungus
    Metarrhizium anisopliae infecting three species of
    larval Elateridae (Coleoptera): IV. Development within
    the host. Can. J. Bot. 17(4):525-534.

Zacharuk, R. Y. 1973. Penetration of the cuticular layers
    of Elaterid larvae (Coleoptera) by the fungus Metarrhizium
    anisopliae, and notes on a bacterial infection. J.
    Invert. Pathol. 21:101-106.